Volume. 7., 2017 ISSN 2253-0371

Annual Review of Chaos Theory, Bifurcations and Dynamical Systems

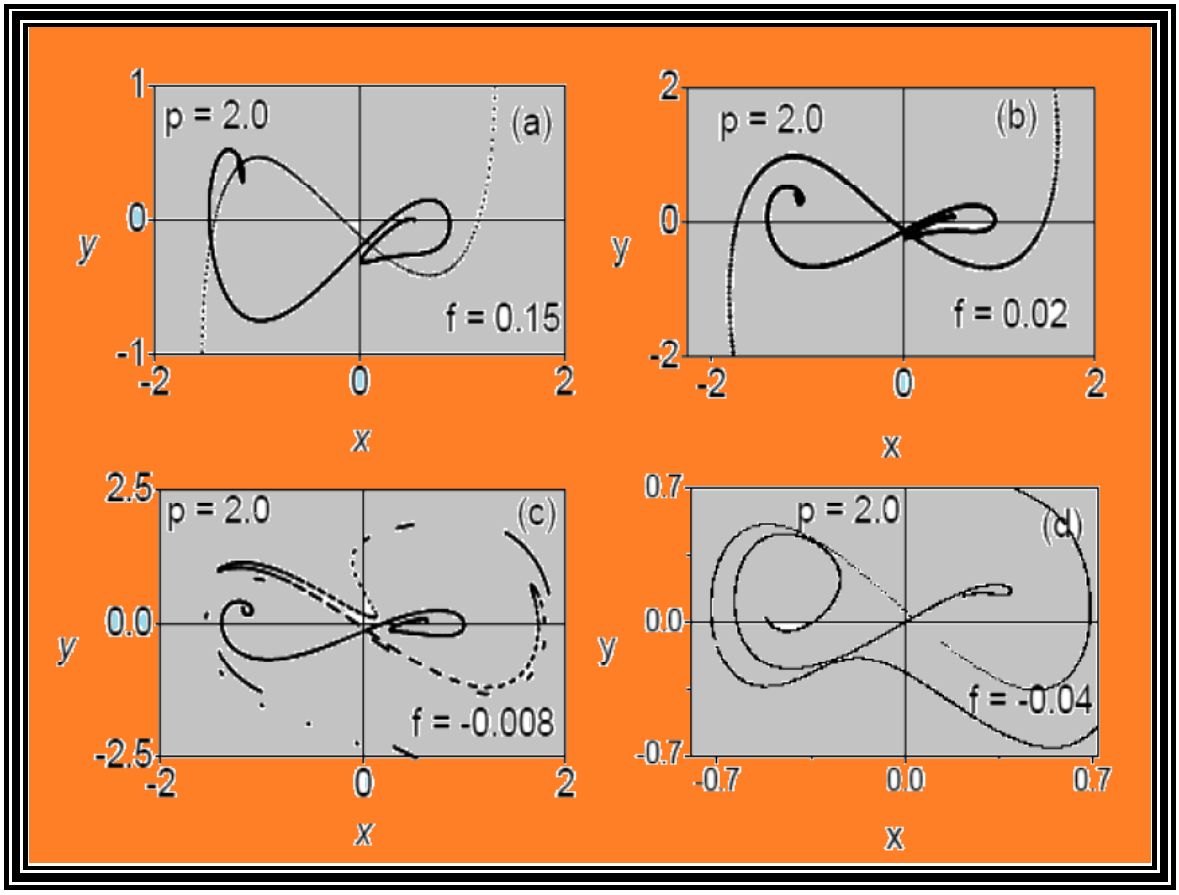

Annual Review of Chaos Theory, Bifurcations and Dynamical Systems

Annual Review of Chaos Theory, Bifurcations and Dynamical Systems

Aims and scope

Annual Review of Chaos Theory, Bifurcations and Dynamical Systems (ARCTBDS) www.arctbds.com) is a multidisciplinary international peer reviewed journal of chaos theory, bifurcations and dynamical systems publishing high-quality articles quarterly. The primary objective of this review journal is to provide a forum for this multidisciplinary discipline of chaos theory, bifurcations and dynamical systems as well as general nonlinear dynamics. This review journal will be a periodical or series that is devoted to the publication of review (and original research) articles that summarize the progress in particular areas of chaos theory, bifurcations and dynamical systems during a preceding period. Also, the journal publishes original articles and contributions on the above topics by leading researchers and developers.

Subject Coverage

Annual Review of Chaos Theory, Bifurcations and Dynamical Systems (ARCTBDS) www.arctbds.com) covers all aspects of chaos theory, bifurcations and dynamical systems. Topics of interest include, but are not limited to:

1. Mathematical modeling, computational methods, principles and numerical simulations.
2. Chaos, bifurcation, nonlinear dynamical systems, complexity in nonlinear science and engineering and numerical methods for nonlinear differential equations.
3. Fractals, pattern formation, solitons, coherent phenomena and nonlinear fluid dynamics.
4. Control theory and stability and singularity on fundamental or applied studies.
5. Real applications in all areas of sciences.

Papers can be oriented towards theory, algorithms, numerical simulations, applications or experimentation.

Readership and audience

Advanced undergraduates and graduate students in natural and human sciences and engineering such as physics, chemistry, biology or bioinformatics…etc; academics and practitioners in nonlinear physics and in various other areas of potential application; researchers, instructors, mathematicians, nonlinear scientists and electronic engineers interested in chaos, nonlinear dynamics and dynamical systems and all interested in nonlinear sciences.

Submission of Papers

Manuscripts should be in English and should be written in a LaTeX file only. All **zelhadj12@yahoo.fr**. The other formats are not acceptable. Authors are advised to keep a copy of their manuscript since the journal cannot accept responsibility for lost copies. The submitted papers to this journal should not have been previously published nor be currently under consideration for publication elsewhere. All papers are refereed through a double blind process. There is no financial reward for reviewers and editors of this journal. These positions are purely voluntary. When the manuscript is accepted for publication, the authors agree to automatic transfer of the copyright to the journal. The manuscript should contain the following items: An informative title, author's name, address and e-mail, abstract, 3-5 keywords, text, conclusion, and references. Footnotes should be avoided. References should appear in alphabetical order and should be denoted in the text by numbers in square brackets, e.g. [10]. References should be complete, in the following style:

- **Papers:** Author(s) initials followed by last name for each author, "paper title," publication name, volume, inclusive page numbers, month and year. Authors should consult Mathematical Reviews for standard abbreviations of journal names..
- **Books:** Author(s), title, publisher, location, year, chapter or page numbers (if desired).
- **Each figure and table or any material** (i.e., FIg 10., Table 1., ...etc) should be mentioned in the text and numbered consecutively using Arabic numerals. Number each table consecutively using Arabic numerals. Type a brief title below each figure and table or any material. Figures should be submitted separately as encapsulated postscript (.eps) files.

For accepted papers, the author(s) will be asked to transfer copyright of the article to the journal. The manuscript will not be published until the **Copyright Transfer Form** is received.

Page proofs will be sent to the corresponding author. The proofs must be corrected and **There are no charges for publishing in this journal and each author will receive a PDF copy of his/her paper.**

Contribution Enquiries and Submitting

ARCTBDS editorial office (Algeria office): Prof. Zeraoulia Elhadj, Department of Mathematics, University of Tébessa, (12002), Algeria, e- zelhadj12@yahoo.fr.

Editorial Board

Editor in Chief

- Zeraoulia Elhadj, Department of Mathematics, University of Tébessa, (12002), Algeria, e- zelhadj12@yahoo.fr.

Annual Review of Chaos Theory, Bifurcations and Dynamical Systems

Volume. 7., 2017

Table of Contents

Annual Review of Chaos Theory, Bifurcations and Dynamical Systems
Vol. 7, (2017) 1-21, www.arctbds.com.

Dynamical behavior of Peter-De-Jong map using the modified 0-1 and 3ST tests for chaos

Thierry Tanze Wontchui
Department of Physics, Faculty of Science, University of Ngaoundéré, Cameroon
e-mail: thierrywontchui@gmail.com

Joseph Yves Effa
Department of Physics, Faculty of Science, University of Ngaoundéré, Cameroon
e-mail: yveseffa@gmail.com

Henri Paul Ekobena Fouda
Laboratoire d'Analyses, Simulations et Essais, IUT, University of Ngaoundéré, Cameroon
e-mail: hekobena@gmail.com

Jean Sire Armand Eyebe Fouda
Department of Physics, Faculty of Science, University of Yaoundé 1, Cameroon
e-mail: efoudajsa@yahoo.fr

Abstract: In this paper, a detailed analysis of the behavior of Peter-De-Jong map using the modified 0-1 and 3ST tests is presented. The results show that both tests work well and effectively distinguish chaotic and regular motions in all the studied cases. The simulation times necessary in all the cases are largely inferior to the ones obtained using the 0-1 test which requires long data sets to perform well. We also performed some comparisons between the 0-1 test and the 3ST test for the litigious cases for which the decision by the 0-1 method is ambiguous, and we claim that the 3ST test can be a good alternative to the 0-1 method. The 3ST test is a very efficient method and is particularly useful in characterizing the quasi-periodic motion.

Keywords: Chaos, 0-1 test, Modified 0-1 test, 3ST test, Peter-De-Jong map.

Manuscript accepted January 20, 2017.

1 Introduction

With the discovery of chaos phenomenon in 1963 by Edward Lorenz [19], the field of nonlinear dynamics has attracted much attention of researchers around the world, leading thus to numerous publications [17, 1]. This phenomenon, owing to its remarkable properties such as ergodicity, extreme sensitivity to initial conditions and control parameters of system, etc. [17, 23], is applying to diverse areas of science as electronic, biology, secure communication, economy, meteorology, etc. Therefore, the determination of regular or chaotic nature of dynamical systems becomes crucial.

Many tools to characterize chaos in these systems have been proposed since long time [1, 2, 9, 14]. We can sort them in two categories: the qualitative methods and quantitative methods. As qualitative method, we can quote: the phase portrait and the bifurcation diagram. This latter is obtained by representing the states of system when one of the control parameters varies. These two techniques just allow us to have a certain idea on the behavior of the system, and are based on visual perception that can prove to be wrong. As quantitative method, we have: the SALI method (Small Alignment Index) [21], the Largest Lyapunov Exponent [24], Entropy [13], the Fast Lyapunov Indicator [8], the Dynamic Lyapunov Indicator [25], the Delay Vector Variance method [15], and so on. However, most of these techniques exhibit practical limitations since they fail to detect chaos for a large class of dynamical systems (non-universality of the tests), require the absolute knowledge of mathematical equations governing the dynamics of the systems (impossibility to handle the experimental data), require a large amount of data which is expensive in computational time, fail to analyze the time series contaminated by noise, complexity of test algorithm, etc. Despite of a lot of efforts devoted, one of the major challenges in the field of characterization of nonlinear dynamical systems remains to propose a test that can overcomes all these limitations.

In a recent past, a new test allowing detection of regular or chaotic nature in deterministic dynamical systems has been proposed by Gottwald and Melbourne, the 0-1 test [10, 12]. It is a binary test which takes in input, the time series data of the deterministic dynamical system and returns 0 or 1 according that the dynamics is respectively regular or chaotic. It does not require the prior knowledge of mathematical equations governing the dynamics of system and the phase space reconstruction which is quite complex [12]. In addition, it is robust to the presence of noise and it is easy to implement. The 0-1 test has been successfully applied to diverse type of system [20, 22, 4, 5, 18] and its reliability has been proved [16, 11]. However, the main disadvantages of this test are: it requires a large amount of data to perform well and its algorithm is based on computing of several multiplications and integrals which are expensive in computation time; it equally fails to detect the nature of the systems when the data are oversampled; the 0-1 test does not also allows distinction between periodic and quasi-periodic behaviors.

In order to overcome the drawbacks of the 0-1 test, two other new tests have recently been proposed by Fouda and his coworkers. These tests are: the modified 0-1 test [6]

and the Three-State test (3ST) [7]. Their reliability should be support by testing them on large and different classes of dynamical systems. In this paper, these two methods are clearly presented and extended to time series data generated by Peter-De-Jong map. We use here this kind of map because it exhibits several complex types of attractors for different set of parameters. The rest of paper is structured as follows: in Section 2, we briefly study the modified 0-1 test. Section 3 is devoted to a detailed study of 3ST test. The Section 4 is consecrated first to the presentation of the Peter-De-Jong map, then we apply the modified 0-1 and 3ST tests to data generated by this map. The results are shown and discussed in this section. Section 5 shows the speed performance of the modified 0-1 and 3ST tests compared to the one of 0-1 test. Finally, Section 6 includes the conclusion of this work.

2 Description of the modified 0-1 test

The modified 0-1 test [6] is a binary test that takes in input the sub-observable and returns 0 or 1 according that the dynamics is respectively regular or chaotic. Here, the sub-observable is defined by mapping exclusively the local maxima and minima (extrema) of the observable. These extrema are computed by detecting the sign changes in the first derivative of the observable. We recall that, the observable is the time series data generated by the underlying dynamical system. This modification does not change the dynamic of system. Therefore if the observable is regular, the sub-observable is also regular and if it is chaotic, the sub-observable remains chaotic. In addition of all the advantages of the traditional 0-1 test, the modified 0-1 test successfully detects chaos in oversampled data [6]. The implementation of modified 0-1 test is given below [6]:
Given an observable $\phi(j)$ with $j = 1, 2, \cdots, N$, we first define the sub-observable $\psi(k)$ with $k = 1, 2, \cdots, L < N$, which is a vector consisting by the local maxima and minima of the entire observable $\phi(j)$. Then, we compute the translations variables $p(n)$ and $q(n)$ of $\psi(k)$. They are defining as

$$p(n) = \sum_{k=1}^{n} \psi(k) \cos(kc) \tag{1}$$

and

$$q(n) = \sum_{k=1}^{n} \psi(k) \sin(kc) \tag{2}$$

where $c \in (0, \pi)$ is the sampling frequency of the time series and $n = 1, 2, \cdots, L$.
The plot of $p - q$ diagram allows us to have a certain idea on the behavior of the system. If the motion is a torus, the dynamic is regular. If it behaves like a Brownian motion, the dynamics is said to be chaotic.

The behavior of $p(n)$ and $q(n)$ can be characterized by computing the mean square displacement (MSD) defined as:

$$M(n) = \lim_{L\to\infty} \frac{1}{L} \sum_{k=1}^{L} [(p(k+n) - p(k))^2 + (q(k+n) - q(k))^2] \tag{3}$$

where $n = 1, 2, \cdots, L/10$.
In order to remove the oscillatory component of $M(n)$, the modified mean square displacement is calculated as follows [12]:

$$D(n) = M(n) - V_{osc}(n) \tag{4}$$

where

$$V_{osc}(n) = E_\psi)^2 \frac{1 - \cos(nc)}{1 - \cos(c)} \tag{5}$$

and

$$E_\psi = \lim_{L\to\infty} \frac{1}{L} \sum_{k=1}^{L} \psi(k) \tag{6}$$

V_{osc} is the oscillatory component of $M(n)$ and E_ψ the average of the sub-observable.
We will use Eq. (4) below to plot the MSD. When this latter is bounded in time, the dynamics of the system is called regular whereas if it grows linearly in time, the dynamics is said to be chaotic.
Finally, we compute the asymptotic growth rate K_c of the MSD on which the test is based. There are two methods to calculate K_c: the regression method and the correlation method. We will use the second method since it allows a better convergence of the asymptotic growth rate. It is given by:

$$K_c = \frac{cov(\xi, \Delta)}{\sqrt{var(\xi)var(\Delta)}} \tag{7}$$

where $\xi = 1, 2, \cdots, L/10$ and $\Delta = D(1), D(2), \cdots, D(L/10)$ are the vectors.
However for some isolated values of c (resonances values), the test fails to detect the dynamics of system. To avoid that, K_c is computed for N_c values of c for a same parameter value ($N_c = 100$, is sufficient in practice); the final asymptotic growth rate K is computed as the median of N_c values of K_c. If $K_c \approx 0$, the dynamics of the system is said to be regular whereas if $K_c \approx 1$ it is known as chaotic.

Despite of the improvement of the 0-1 test, the modified 0-1 test does not allow to distinguish between periodic and quasi-periodic motions. In order to overcome this limitation, another test for chaos detection in discrete dynamical systems has been proposed; it is the 3ST test.

3 Description of the three state test (3ST)

The 3ST test [7] is another technique that allows chaos detection in discrete dynamical systems. It is based on the pattern analysis of data series. It studies the distribution of the system states in a data series as a function of time. The 3ST considers the properties of periodic and quasi-periodic signal for determining whether the dynamics of a system is regular or chaotic [7]. In addition to the afore-mentioned advantages of the 0-1 test, the 3ST test has been developed to make a clear distinction between periodic, quasi-periodic and chaotic behaviors; it has also been developed for real time application due to the fact that its implementation most use addition and subtraction operators; and finally for automating the detection of the period doubling route to chaos. The implementation of 3ST test is shown below [7]:
given an observable to be characterized $x_j(k) = \Phi(x(k))$ with $k \in \mathbb{N}$, $x(k) = (x_1, x_2, \cdots, x_M)(k)$ the state vector, $1 \leq j \leq M$; for determining its patterns, we define $u_j = g(x_j)$ which is the time series data sorted by ascending order with g a function; then we also define $v_j = q(u_j) = q(g(x_j))$ representing the distribution of indices outputting the initial positions of the values of u_j in x_j.
In order to take into account the time dependence of $v_j(k, N)$ (N being the length of time series data), the largest slope (LS) is defined as pattern characteristic as follows:

$$LS(n) = \max_{1 \leq k \leq N-1} (v_j(k+1, N) - v_j(k, N)) \tag{8}$$

It is then possible to use its mean square error $\sigma_{LS}(N, n)$ for chaos detection in time series data as follows:

$$\sigma_{LS}(N, n) = \sqrt{\frac{1}{N} \sum_{j=0}^{p} (LS(jN_0 + n) - \overline{LS})^2} \tag{9}$$

with

$$\overline{LS} = \frac{1}{N} \sum_{j=1}^{p} LS(jN_0 + n) \tag{10}$$

where $N = pN_0 + n$ is the length of data series, N_0 the integration step and p a natural number different from zero. $\sigma_{LS}(N, n)$ measures the ability of a dynamical system to generate new patterns as the time is increasing. n is the smallest observation duration for the LS to be well evaluated and should verify the relation $n \ll N$. According to the behavior of LS, $\sigma_{LS}(N, n)$ is bounded if the underlying dynamics is non chaotic. For this purpose, we define

$$\mu(N, n) = \frac{\log(1 + \sigma_{LS}(N, n))}{\log N} \tag{11}$$

then

$$K(n) = \lim_{n \to +\infty} \mu(N, n) \tag{12}$$

K is the asymptotic growth rate of the mean square error of LS. K is equal to zero in the case of periodic and quasi-periodic motions and greater than zero in the case of chaotic motion.

In order to distinguish periodic from quasi-periodic motions, the global derivative of $\mu(N, n)$ is computed. Its sign can then allow distinguishing these two behaviors. This global derivative is defined as:

$$\lambda(n) = \lim_{n \to +\infty} \sum_{k=1}^{m-1} (\mu(N_{k+1}, n) - \mu(N_k, n)) \tag{13}$$

where $N_1 \ll N_m$. N_1 is the smallest integration duration and N_m is the greatest one. In practice, choose the time delay $n \leq N_1/2$ leads to good results. λ is the periodicity index and allows characterizing regular and chaotic dynamics. The 3ST test is based on its sign: $\lambda(n) < 0$ for quasi-periodic behavior, $\lambda(n) = 0$ for periodic behavior and $\lambda(n) > 0$ for chaotic behavior. Thus, the 3ST as indicated by its name allows to have in output three main parameters which are: L the cycle of periodic orbits, K the asymptotic growth rate of the largest slope and λ the periodicity index.

Moreover, 3ST like other chaos detection tools is extremely sensitive to small change in the input time series. To make it more robust to the presence of noise, an absolute threshold α has been introduced on the input time series such that two states $\tilde{x}(k)$ and $\tilde{x}(j)$ are assumed to be different if and only if $|\tilde{x}(k) - \tilde{x}(j)| \geq \alpha$. The effectiveness of the studied tests is shown by applying them to time series data generated from the Peter-De-Jong map.

4 Peter-De-Jong map: Application of the modified 0-1 and 3ST tests

The Peter-De-Jong map is a pair of difference equations suggested by Peter-De-Jong and so named after him [3]. It is a chaotic system that appears simple, but exhibiting several complex types of attractors, corresponding to different sets of parameters. The map is described as:

$$\begin{cases} x_{n+1} &= \sin(ay_n) - \cos(bx_n) \\ y_{n+1} &= \sin(cx_n) - \cos(dy_n) \end{cases} \tag{14}$$

where a, b, c and d are the parameters of the system.
Below, different sets of these parameters are presented. For each set, we evolved the map (Eq. (14)) and analyzed the obtained time series data through the modified 0-1 and 3ST tests. The results are compared to those of the ordinary 0-1 test and phase portrait plot as shown in Fig. 1 to Fig. 10 below. Also, the values of K by 0-1 test, K_{mod} by modified 0-1 test, K_{3ST} and λ for 3ST are given for each set of parameters. We used an input

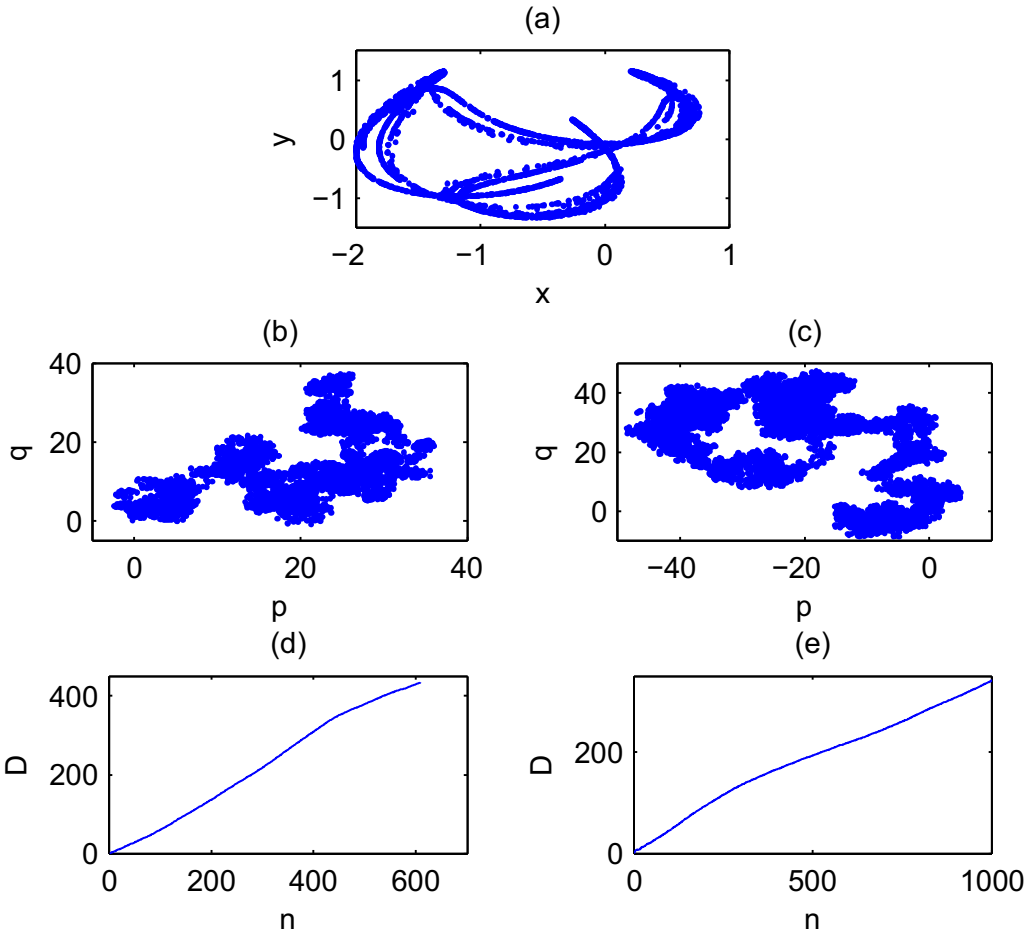

Figure 1: Plot of (a) phase portrait, (b) p-q diagram for the modified 0-1 test, (c) p-q diagram for the 0-1 test, (d) mean square displacement for the modified 0-1 test and (e) mean square displacement for the 0-1 test. The parameter values are: $a = 2.033372$, $b = -0.78980076$, $c = -0.5964787$, $d = -1.7829015$. $K = 0.9974$; $K_{mod} = 0.9988$; $K_{3ST} = 0.8225$; $\lambda = 0.0983$.

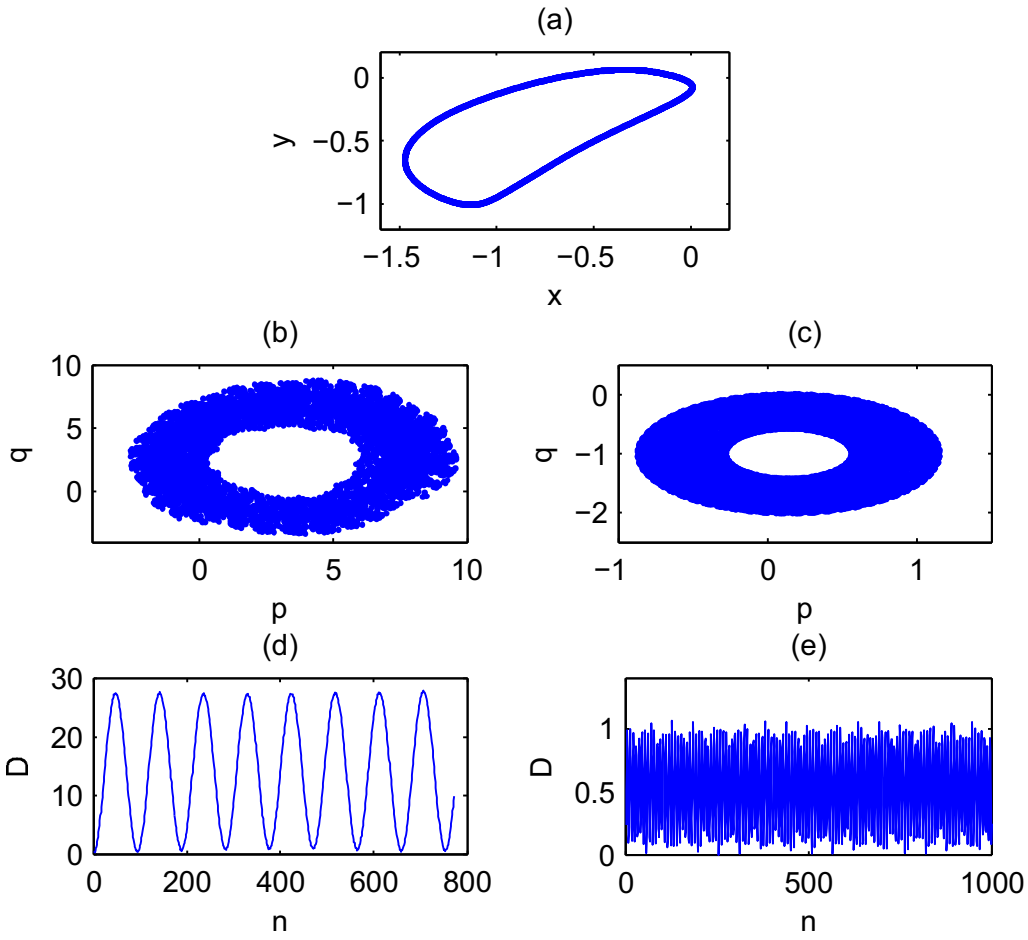

Figure 2: Plot of (a) phase portrait, (b) p-q diagram for the modified 0-1 test, (c) p-q diagram for the 0-1 test, (d) mean square displacement for the modified 0-1 test and (e) mean square displacement for the 0-1 test. The parameter values are: $a = 1.76$, $b = 1.66571$, $c = -0.86114$, $d = 0.59714$. $K = -0.0055$; $K_{mod} = -0.0668$; $K_{3ST} = 0.4537$; $\lambda = -0.0617$.

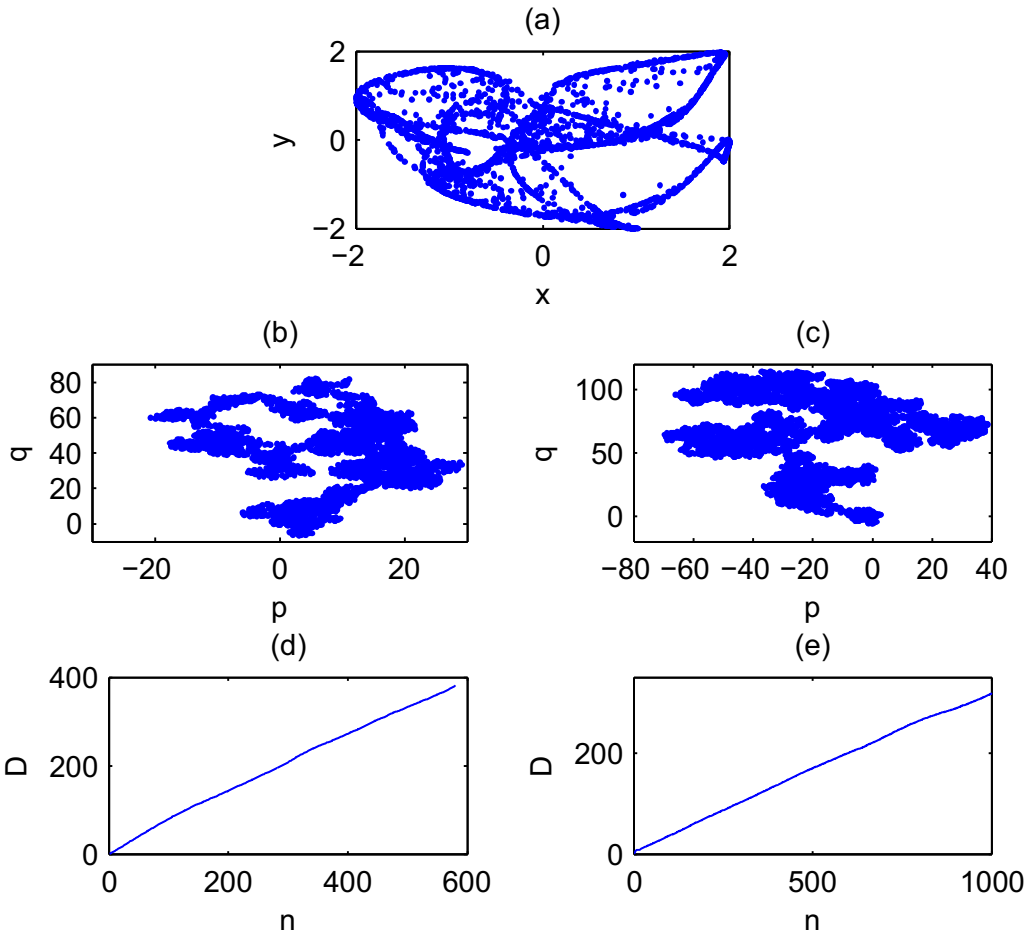

Figure 3: Plot of (a) phase portrait, (b) p-q diagram for the modified 0-1 test, (c) p-q diagram for the 0-1 test, (d) mean square displacement for the modified 0-1 test and (e) mean square displacement for the 0-1 test. The parameter values are: $a = 0.973894$, $b = 1.66504$, $c = -0.860796$, $d = 2.10487$. $K = 0.9937$; $K_{mod} = 0.9991$; $K_{3ST} = 0.8211$; $\lambda = 0.1015$.

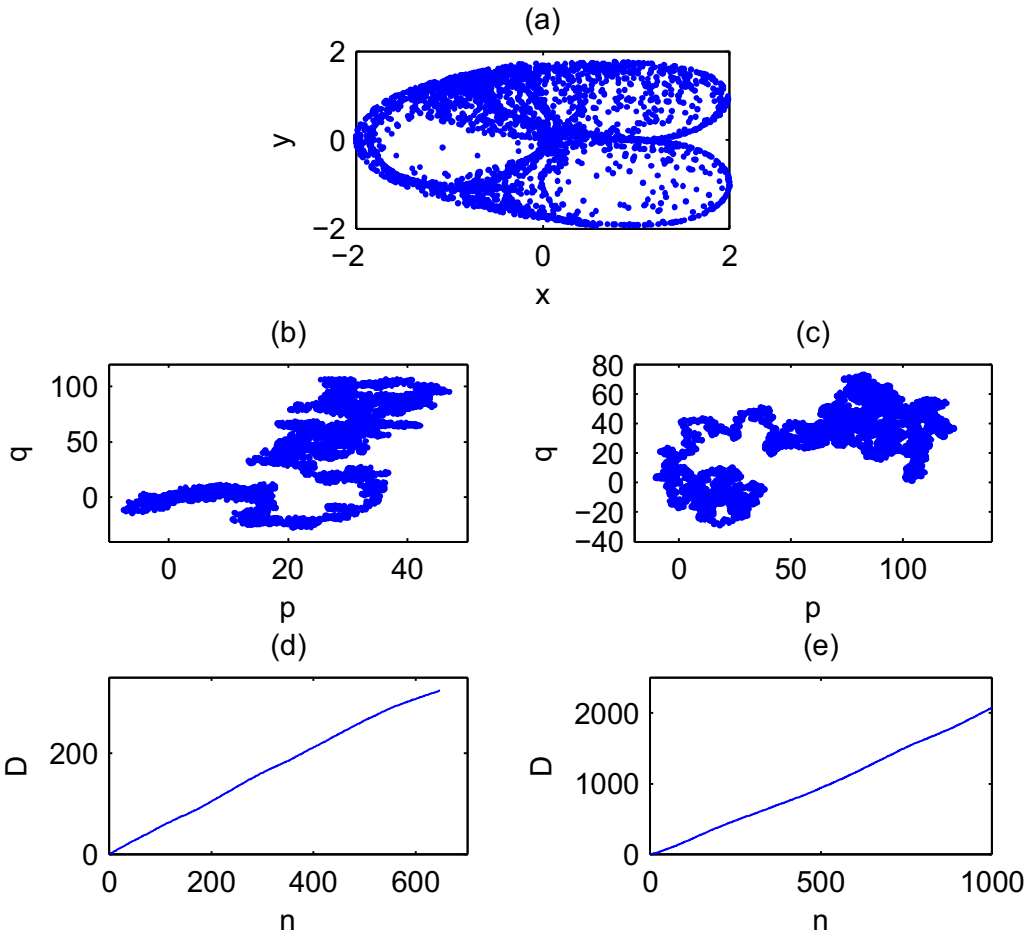

Figure 4: Plot of (a) phase portrait, (b) p-q diagram for the modified 0-1 test, (c) p-q diagram for the 0-1 test, (d) mean square displacement for the modified 0-1 test and (e) mean square displacement for the 0-1 test. The parameter values are: $a = 2.07345$, $b = 1.66504$, $c = -0.860796$, $d = 2.10487$. $K = 0.9996$; $K_{mod} = 0.9905$; $K_{3ST} = 0.8263$; $\lambda = 0.0953$.

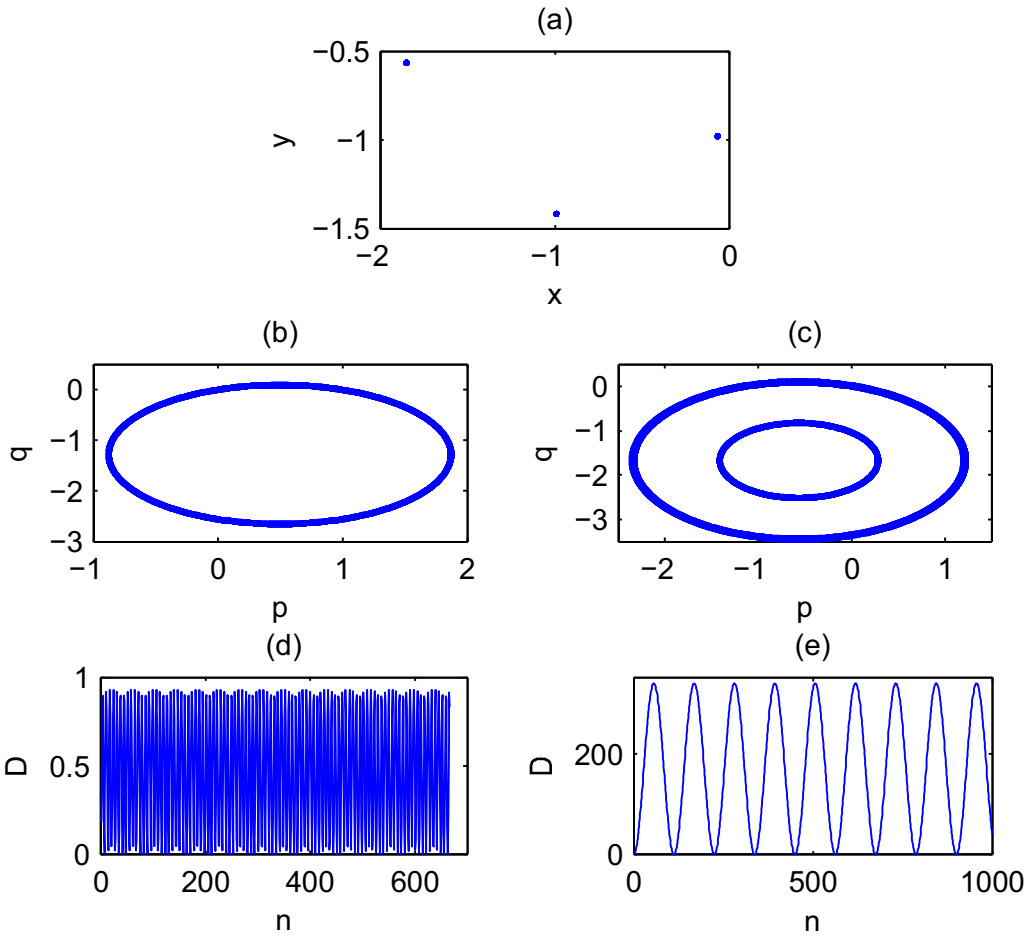

Figure 5: Plot of (a) phase portrait, (b) p-q diagram for the modified 0-1 test, (c) p-q diagram for the 0-1 test, (d) mean square displacement for the modified 0-1 test and (e) mean square displacement for the 0-1 test. The parameter values are: $a = 1.07345$, $b = 2.785398$, $c = 1.34786$, $d = 1.10487$. $K = -0.0033$; $K_{mod} = -0.00015$; $K_{3ST} = 0$; $\lambda = 0$.

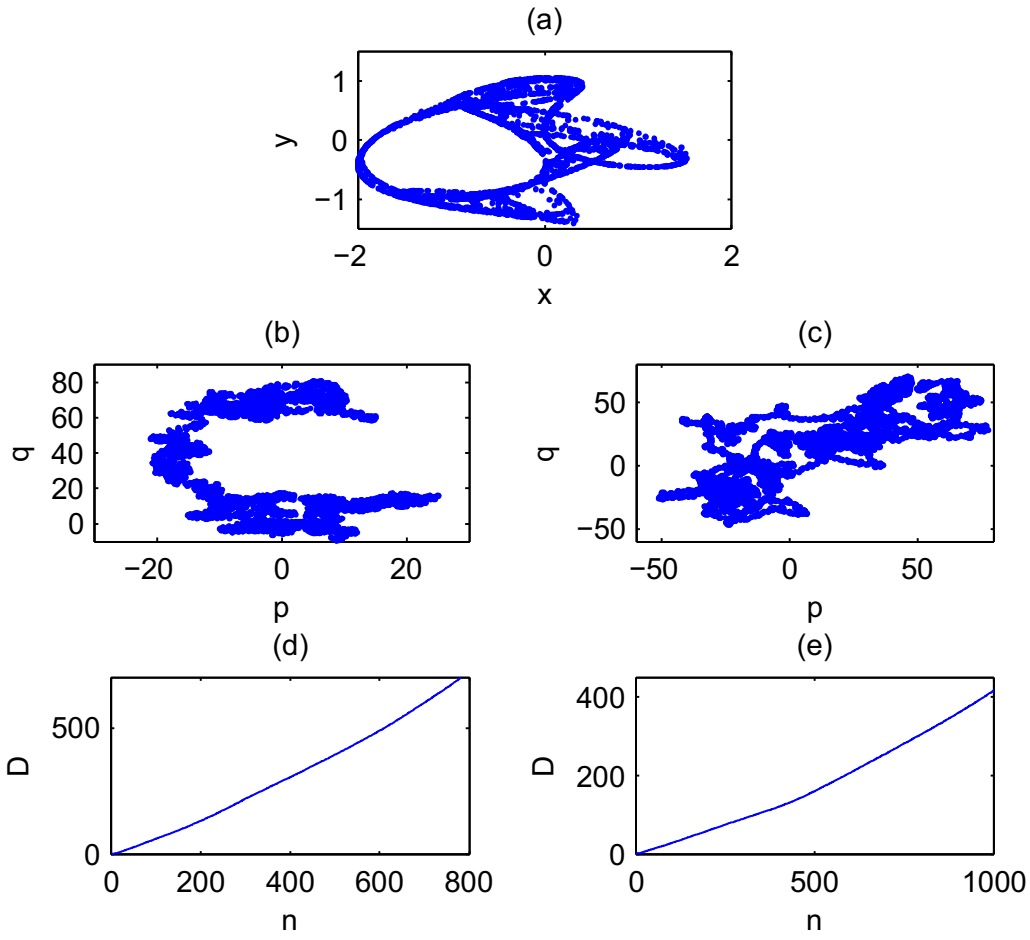

Figure 6: Plot of (a) phase portrait, (b) p-q diagram for the modified 0-1 test, (c) p-q diagram for the 0-1 test, (d) mean square displacement for the modified 0-1 test and (e) mean square displacement for the 0-1 test. The parameter values are: $a = 2.89027$, $b = 1.5708$, $c = -0.314159$, $d = 2.10487$. $K = 0.9950$; $K_{mod} = 0.9821$; $K_{3ST} = 0.8241$; $\lambda = 0.0966$.

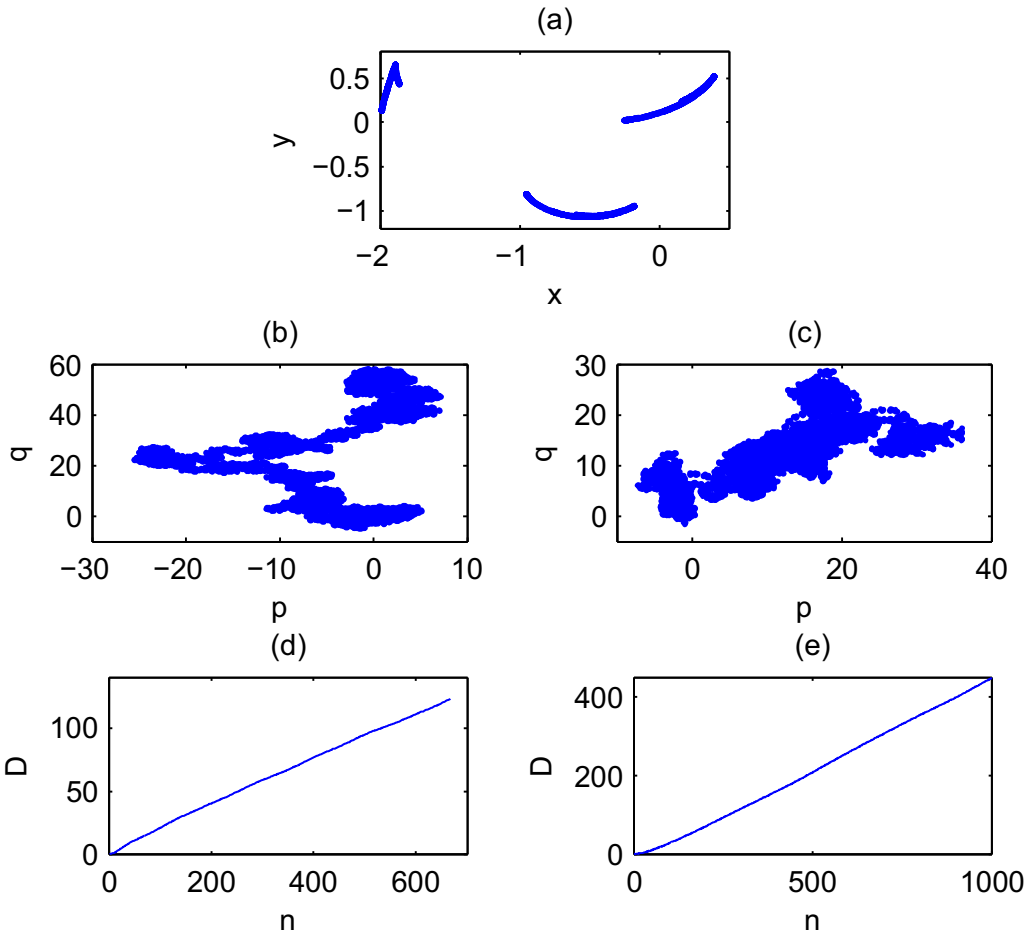

Figure 7: Plot of (a) phase portrait, (b) p-q diagram for the modified 0-1 test, (c) p-q diagram for the 0-1 test, (d) mean square displacement for the modified 0-1 test and (e) mean square displacement for the 0-1 test. The parameter values are: $a = 1.7843$, $b = 0.5366543$, $c = -0.7553879$, $d = 1.65469$. $K = 0.8975$; $K_{mod} = 0.9872$; $K_{3ST} = 0.8164$; $\lambda = 0.0911$.

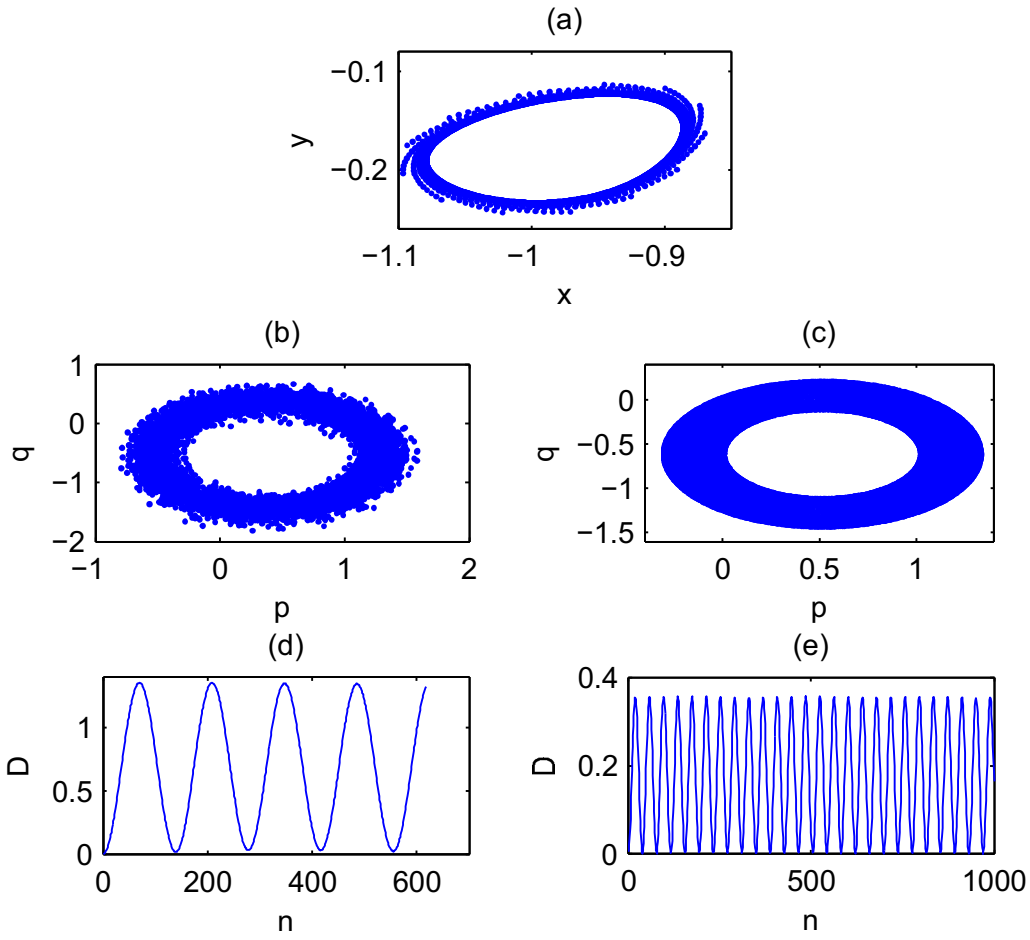

Figure 8: Plot of (a) phase portrait, (b) p-q diagram for the modified 0-1 test, (c) p-q diagram for the 0-1 test, (d) mean square displacement for the modified 0-1 test and (e) mean square displacement for the 0-1 test. The parameter values are: $a = 1.7843$, $b = 0.8574$, $c = -0.975840$, $d = 0.65469$. $K = -0.0011$; $K_{mod} = 0.0092$; $K_{3ST} = 0$; $\lambda = 0$.

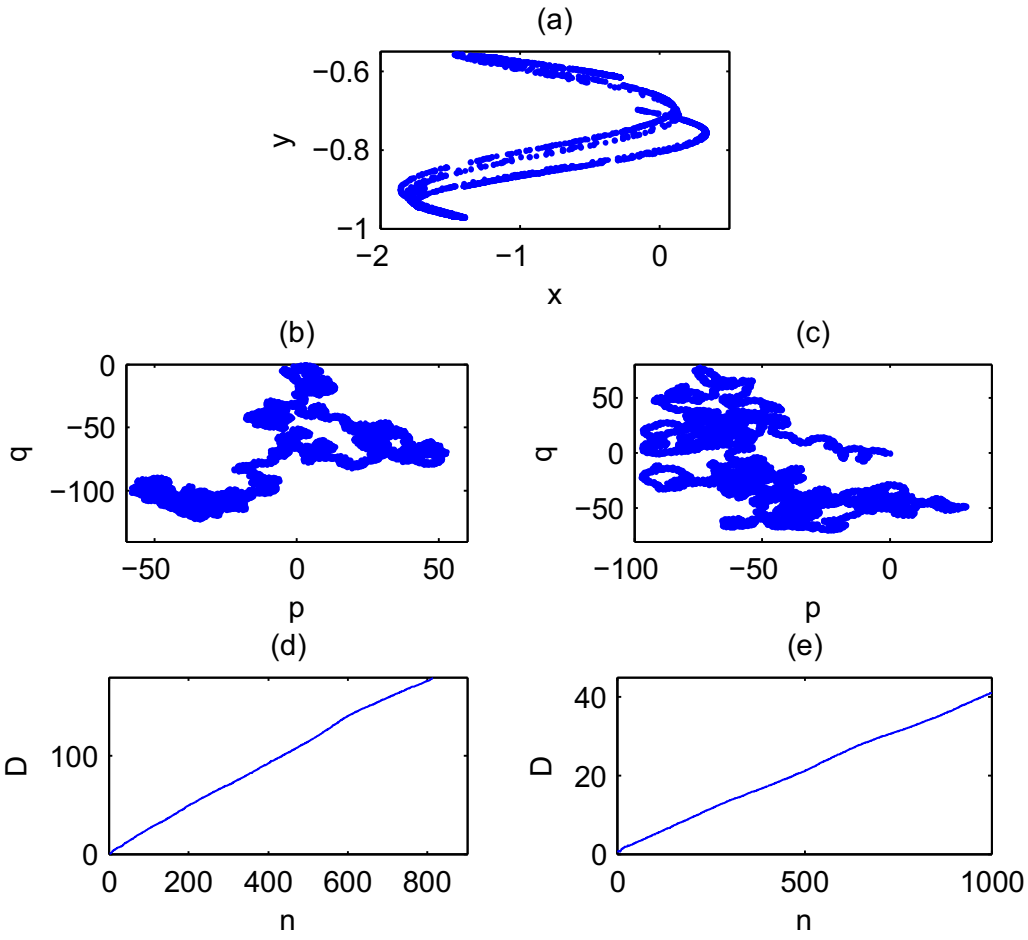

Figure 9: Plot of (a) phase portrait, (b) p-q diagram for the modified 0-1 test, (c) p-q diagram for the 0-1 test, (d) mean square displacement for the modified 0-1 test and (e) mean square displacement for the 0-1 test. The parameter values are: $a = 1.273574$, $b = 2.8574$, $c = -0.175345$, $d = 0.55469$. $K = 0.9972$; $K_{mod} = 0.9962$; $K_{3ST} = 0.8241$; $\lambda = 0.0770$.

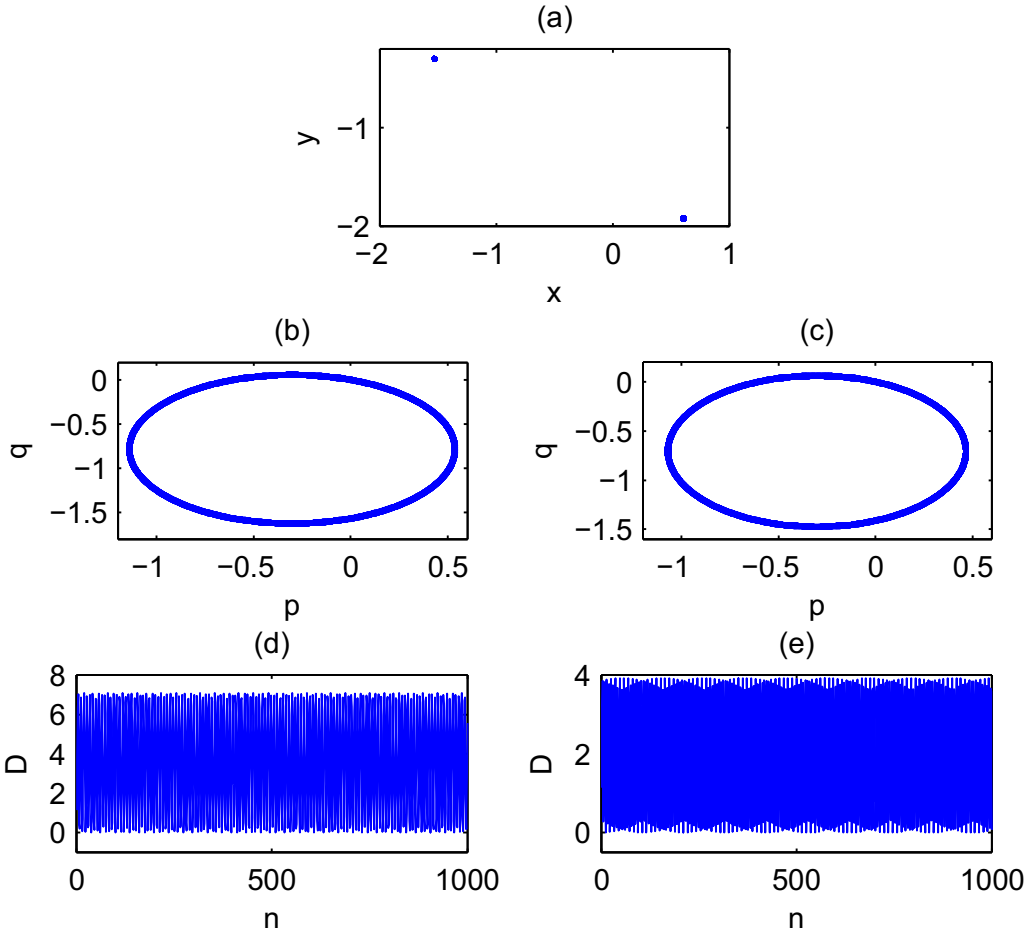

Figure 10: Plot of (a) phase portrait, (b) p-q diagram for the modified 0-1 test, (c) p-q diagram for the 0-1 test, (d) mean square displacement for the modified 0-1 test and (e) mean square displacement for the 0-1 test. The parameter values are: $a = 0.76453$, $b = 1.66571$, $c = 1.28857$, $d = 0$. $K = 0.00042$; $K_{mod} = -0.00058$; $K_{3ST} = 0$; $\lambda = 0$.

sequence of length $N = 2000$ for the 3ST algorithm and $N = 10000$ for the 0-1 and the modified 0-1 tests.

The results show that for the cases of Fig. 1, Fig. 3, Fig. 4 and Fig. 6, the phase portrait plot seems to be chaotic (Fig. 1(a), Fig. 3(a), Fig. 4(a), Fig. 6(a)). This chaotic nature is confirmed by the Brownian motion of the p-q diagrams (Fig. 1(b),(c); Fig. 3(b),(c); Fig. 4(b),(c); Fig. 6(b),(c)), the linear growth of the MSD (Fig. 1(d),(e); Fig. 3(d),(e); Fig. 4(d),(e); Fig. 6(d),(e)), the parameters values K_{mod} and K_{0-1} which are approximately 1 for the modified 0-1 test and the 0-1 test as presented on these Figures. Besides, the parameters values K_{3ST} and λ_{3ST} by 3ST are greater than 0.

For the cases of Fig. 5, Fig. 8 and Fig. 10, the phase plot appears to be regular (Fig. 5(a), Fig. 8(a), Fig. 10(a)). This regular nature is confirmed by the torus motion of the p-q diagrams (Fig. 5(b),(c); Fig. 8(b),(c); Fig. 10(b),(c)), the bounded behavior of the MSD (Fig. 5(d),(e); Fig. 8(d),(e); Fig. 10(d),(e)), the parameters values K_{mod} and K_{0-1} that are close to 0 for the modified 0-1 test and 0-1 test. Also, the parameters values K_{3ST} and λ_{3ST} by 3ST are equal to 0.

In regard to the Fig. 7 and Fig. 9, the phase portrait plot does not appears to be chaotic while the modified 0-1 test, the 0-1 test and the 3ST detect chaos for these parameters. So for these cases, the phase portrait fails to detect chaos. We can explain by the fact that it is based on the visual perception which can be wrong; also, the chaos presented by the map for these parameters may be weak.

For the case of Fig. 2, the phase portrait plot seems to be regular; this regular nature is also detected by the modified 0-1 and 0-1 tests. However both tests indicate the periodic motion. The 3ST being less sensitive to the sequence of input times series generated by the system, the value of the periodicity index is $\lambda_{3ST} = -0.0617$, which may be interpreted as quasi-periodic motion. This test is a very efficient method and is particularly useful in characterizing the quasi-periodic motion.

To better characterize the behavior of the Peter-De-Jong map when a control parameter varies with the time, its global dynamics is valued using the modified 0-1 and 3ST tests for parameter value a varying from -5 to 5, with $b = -0.78980076$, $c = -0.5964787$ and $d = -1.7829015$. The results are compared with those of the 0-1 test and the bifurcation diagram as displayed in Fig. 11 below. As shown in Fig. 11, the results of the modified 0-1 and 3ST tests are in good agreement with those of the bifurcation diagram and the 0-1 test for most part of points in the range of variation of the control parameter. Nevertheless in some short ranges at $a \approx [-4, -3.8]$ and $a \approx [1, 1.2]$, the dynamics seem to be litigious. It is difficult to take a decision regarding the dynamics of the system by only visualizing the bifurcation diagram (Fig. 11(a)). The dynamics there might be quasi-periodic or weakly chaotic. In these small ranges the 0-1 test detects a regular dynamics (Fig. 11(b)) while the modified behaves as a weak chaos (Fig. 11(c)). The 3ST detects quasi-periodicity in some points of these ranges (Fig. 11(e)).

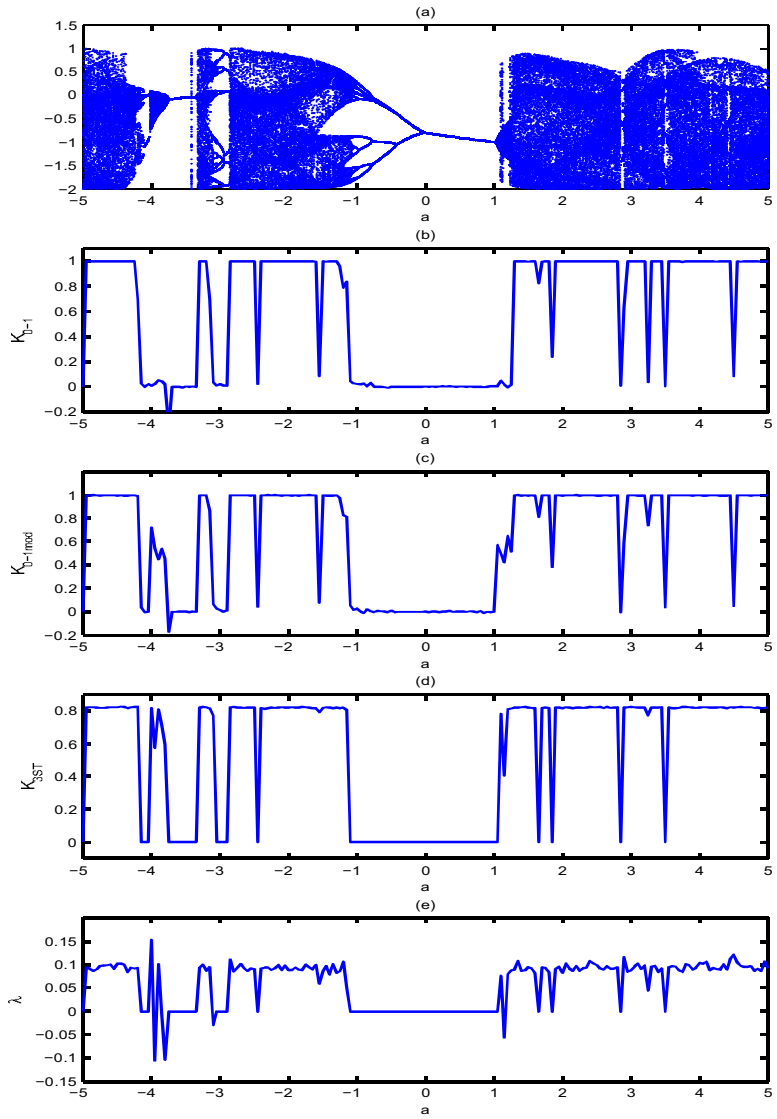

Figure 11: Global dynamics of the Peter-De-Jong map for control parameter a varying from -5 to 5: (a) bifurcation diagram, (b) asymptotic growth rate K_{0-1} by 0-1 test, (c) asymptotic growth rate K_{mod} by modified 0-1 test, (d) asymptotic growth rate K_{3ST} by 3ST test and (e) periodicity index λ_{3ST} by 3ST test.

5 Speeds analysis

For an efficient using of chaos detection methods for applications in areas of science, we must be able to process the data in real time. For this purpose, we propose to compare the processing speeds of the above studied tests for chaos detection. All the operations are implemented using Matlab 7.9.0 (R2009b) on a personal computer equipped with an Intel(R) Core(TM) i3-M370, 2.40 GHz CPU, running Windows 7.

In regard to the cases 1 to 10 (Fig. 1 to Fig. 10), the average simulation time for each case is around $35s$ for the modified 0-1 test; $84s$ for the 0-1 test and $0.1s$ for the 3ST test. We notice that the computation time of the modified 0-1 test is 2.4 times lower than the one of the 0-1 test and 350 times greater than the one of the 3ST test. So the simulation time of the 3ST test is quite inconsiderable compared to those of others tests. The simulation time of the modified 0-1 test is significantly reduced since the number of data to be processed is reduced. For example, if the time series to analyze is a sinusoid, we just process its maximum and minimum instead to process all points of the sinusoid. Nevertheless, despite of fact that the computation time of the modified 0-1 test compared to ordinary 0-1 test is considerably reduced, this time remains again heavy.

For the simulation time of global dynamics of the Peter-De-Jong map, we obtained $8064s$ approximately 2.24 hours for the modified 0-1 test and $11139s$ approximately 3.0942 hours for the 0-1 test. Although this time is reduced for the modified 0-1 test, it still remains quite large compared to the one of 3ST test that has been assessed to around $21s$. Thus the 3ST test is expected to process experimental data in real time.

6 Conclusion

Chaos detection in dynamical systems is a nontrivial problem. In order to generalize a method, it is important to prove its reliability. In this paper, a detailed study of the behavior of Peter-De-Jong map using two chaos detection methods namely the modified 0-1 and 3ST tests was performed. Regarding the modified 0-1 test, it consists to process only the local maxima and minima of time series data rather than treat the entire observable like the ordinary 0-1 test. The 3ST test is based on pattern analysis of time series data. These two tests for chaos do not require the knowledge of the mathematical equations governing the dynamics of system to be applied as well as the nature and the dimension of the underlying vector field. To show the effectiveness and the reliability of these tests, we must applied them to data generated by various dynamical systems. Therefore, in this work we have applied them to time series generated from the Peter-De-Jong map. The results showed that the modified 0-1 and 3ST tests perform well for all cases of parameters. These two tests for chaos have then shown their applicability to this kind of map. The paper also shows that the 3ST test can be a better alternative to 0-1 test and classical methods as it detects quasi-periodic motion in the map where the others tests fail. Based on the time that has allowed us to simulate the global dynamics of the

Peter-De-Jong map, we can say that the 3ST can be used to process experimental data in real time. In prospect, we plane to apply the 3ST test to real world data.

References

[1] M. Barahona and C.-S. Poon. Detection of nonlinear dynamics in short, noisy time series. *Nature*, 3(81):215–217, 1996.

[2] S. Basu and E. Foufoula-Georgiou. Detection of nonlinearity and chaoticity in time series using the transportation distance function. *Phys. Lett. A*, 301(5-6):413–423, 2002.

[3] M. Budhraja, N. Kumar, and L. M. Saha. The 0-1 test applied to peter-de-jong map. *Int. J. Eng.Innov. Tech.*, 2(6):253–257, 2012.

[4] J. H. P. Dawes and M. C. Freeland. The '0-1 test for chaos' and strange nonchaotic attractors. `http://people.bath.ac.uk/jhpd20/publications/sna.pdf`, 2008.

[5] I. Falconer, G. A. Gottwald, I. Melbourne, and K. Wormnes. Application of the 0-1 test for chaos to experimental data. *SIAM J. Appl. Dyn.*, 6:395–402, 2005.

[6] J. S. A. E. Fouda, B. Bodo, S. L. Sabat, and J. Y. Effa. A modified 0-1 test for chaos detection in oversampled times series observations. *Int. J. Bifurc. Chaos*, 24(5):1450063, 2014.

[7] J. S. A. E. Fouda, J. Y. Effa, M. Kom, and M. Ali. The three-state test for chaos detection in discrete maps. *Appl. Soft Comput.*, 13(12):4731–4737, 2013.

[8] C. Froeschlé, E. Lega, and Gonczi R. Fast lyapunov indicators: Application to asteroidal motion. *Celest. Mech. Dyn. Astron.*, 67(1):41–62, 1997.

[9] J. F. Gemmeke, S. F. Portegies Zwart, and C. J. H. Kruip. Detecting irregular orbits in gravitational n-body simulations. *Commun. Nonlinear Sci. Numer. Simulat.*, 13(6):1157–1168, 2008.

[10] G. A. Gottwald and I. Melbourne. A new test of chaos in deterministic systems. *Proc. Roy. Soc. A*, 460:603–611, 2004.

[11] G. A. Gottwald and I. Melbourne. Comment on reliability of the 0-1 test for chaos. *Phys. Rev. E*, 77:028201, 2008.

[12] G. A. Gottwald and I. Melbourne. On the implementation of the 0 1 test for chaos. *SIAM J. Appl. Dyn. Syst.*, 8:129–145, 2008.

[13] P. Grassberger and I. Procaccia. Characterization of strange attractors. *Phys. Rev. Lett.*, 50(5):346–349, 1983.

[14] W. Heng-Dong, L. Li-Ping, and G. Jian-Xiu. An efficient method of distinguishing chaos from noise. *Chin. Phys. B*, 19(5):050505, 2010.

[15] S. Hou, Y. Li, and S. Zhao. Detecting the nonlinearity in time series from continuous dynamic systems based on delay vector variance method. *Int. J. Math. Computer Sci. Eng.*, 1(2):41–46, 2007.

[16] J. Hu, W.W. Tung, J. Gao, and Y. Cao. Reliability of the 0-1 test for chaos. *Phys. Rev. E*, 72:056207, 2005.

[17] M. S. Jakimoski and L. Kocarev. Chaos and cryptography. *IEEE Trans. Circ. Syst. I: Fund. Theory Appl.*, 48(2):163–169, 2001.

[18] G. Litak, A. Syta, and M. Wiercigroch. Identification of chaos in a cutting process by the 0-1 test. *Chaos, Solitons and Fractals*, 40:2095–2101, 2009.

[19] E. N. Lorenz. Deterministic nonperiodic flow. *J. Atmosph. Sci.*, 20(2):130–141, 1963.

[20] M. A. Maysoon and N. F. Mansour. Numerical and chaotic analysis of chuas circuit. *J. Emerging Trends Comput. Information Sci.*, 3:783–791, 2012.

[21] C. Skokos. Alignment indices: A new, simple method for determining the ordered and chaotic nature of orbits. *J. Phys. A*, 34(47):10029–10043, 2001.

[22] C. Skokos, C. Antonopoulos, T. C. Bountis, and M. N. Vrahatis. Detecting order and chaos in hamiltonian system by the sali method. *J. Phys. A*, 37:6269–6284, 2004.

[23] S. H. Strogatz. *Nonlinear Dynamics and Chaos with applications to Physics, Biology, Chemistry, and Engineering.* Perseus books publishing, 1994.

[24] A. Wolf, J. B. Swift, H. L. Swinney, and J. A. Vastano. Determining lyapunov exponents from a time series. *Physica D*, 16(3):285–317, 1985.

[25] M. Yuasa and L. M. Saha. Indicators of chaos. `https://www.google.cm/?gws_rd=cr,ssl&ei=BmxBWO6IBsm7UfX4iegJ#q=+Manabu+Yuasa+and+L.+M.+Saha+%2B+indicators+of+chaos+2007+pdf`, 2008.

Annual Review of Chaos Theory, Bifurcations and Dynamical Systems
Vol. 7, (2017) 22-40, www.arctbds.com.

Limits of Solutions of a Recurrence Relation with Bang Bang Control

Jiannan Song

Department of mathematics, Yanbian university, Yanji 133002, China

e-mail: 2144011786@ybu.edu.cn

Fan Wu
Department of mathematics, Yanbian university, Yanji 133002, China
e-mail: fwu1994@ybu.edu.cn

Chengmin Hou
Department of mathematics, Yanbian university, Yanji 133002, China
e-mail: cmhou@foxmail.com

Abstract: In this paper, we consider a three term nonlinear recurrence $x_n = ax_{n-2} + bH(x_{n-1}) + c$ where $a > 0$ and b, c are real numbers and H is the Heaviside step function. We are able to derive the exact relations between the initial values x_{-2} and x_{-1} with the limiting behaviors of the solution determined by them. In particular, when $a \in (0, 1)$ and $b > 0$, we are able to show that all solutions $\{x_k\}_{k=-2}^{\infty}$ converge if, and only if, (i) $(c + b)/(1 - a) < 0$, (ii) $(c - b)/(1 - a) > 0$, (iii) $(c + b)/(1 - a) = 0$ and $x_{-2}, x_{-1} \in \mathbf{R}^-$; or, (iv) $(c - b)/(1 - a) = 0$ and $x_{-2}, x_{-1} \in \mathbf{R}^+$.

Keywords: Three term nonlinear recurrence, Heaviside function, limiting behavior.

Manuscript accepted January 20, 2017.

1 Introduction

Three term recurrence relations of the form

$$y_n = F(y_{n-1}, y_{n-2}),\ n \in \mathbf{N} = \{0, 1, 2, 3, ...\},$$

arise in many studies of natural phenomena. A well known example is the relation

$$y_n = y_{n-1} + y_{n-2},\ n \in \mathbf{N},$$

which is satisfied by the Fibonacci sequence $\{0, 1, 1, 2, 3, 5, 8, ...\}$. When F is a continuous function in the above recurrence relation, there are now numerous studies, but when F is discontinuous, relatively few studies are available (see e.g. [1–4]). However, (discontinuous) on-off control functions such as

$$H(u) = \begin{cases} 1, & u \le 0 \\ -1, & u > 0 \end{cases},\ G(u) = \begin{cases} 1, & u \ge 0 \\ -1, & u < 0 \end{cases}, \tag{1}$$

or

$$H_\lambda(u) = \begin{cases} 1, & u \le \lambda \\ -1, & u > \lambda \end{cases},\ \lambda \in \mathbf{R}, \tag{2}$$

etc. are common and therefore it is of great importance to consider prototype models and study their properties.

In this paper, we consider the following recurrence relation

$$y_n = ay_{n-2} + bH_\lambda(y_{n-1}) + c,\ n \in \mathbf{N}, \tag{3}$$

where $a \in (0, +\infty), b, c \in \mathbf{R}$ and $H_\lambda : \mathbf{R} \to \mathbf{R}$ is the bang bang function defined by (2). Clearly, given any initial pair (y_{-2}, y_{-1}) in $\mathbf{R}^2$, we can generate through (3) a unique real sequence $\{y_n\}_{n=-2}^{\infty}$. Such a sequence is called a solution of (3) originated from (y_{-2}, y_{-1}).

There are many qualitative properties of this nonlinear recurrence which are worthy of studying. Here, we are interested in the limit of the solution sequence $\{y_n\}_{n=-2}^{\infty}$ originated from $\mathbf{R}^2$.

As we will see below, there are only a few types of limiting behaviors for solutions of (3) and we can also determine exactly the 'initial region' from which each type of solutions originate from.

Since there are four real parameters in the nonlinear model (3), the above precise information may seem difficult. Fortunately, we may resort to linear recurrences and transformations for help.

Indeed, let $\{y_k\}_{k=-2}^{\infty}$ be real sequences that satisfy

$$y_{2k} = ay_{2k-2} + d,\ k \in \mathbf{N}, \tag{4}$$

$$y_{2k+1} = ay_{2k-1} + d,\ k \in \mathbf{N}, \tag{5}$$

where $a \in (0, +\infty)$ and d is a real number. Then the following facts are easily obtained by induction.

- If $a \neq 1$ and $\{y_n\}_{n=-2}^{\infty}$ is a sequence which satisfies (4), then

$$y_{2k} = a^{k+1} y_{-2} + \frac{(1 - a^{k+1})}{1 - a} d, \ k \in \mathbf{N}. \tag{6}$$

- If $a \neq 1$ and $\{y_n\}_{n=-2}^{\infty}$ is a sequence which satisfies (5), then

$$y_{2k+1} = a^{k+1} y_{-1} + \frac{(1 - a^{k+1})}{1 - a} d, \ k \in \mathbf{N}. \tag{7}$$

- If $a = 1$ and $\{y_n\}_{n=-2}^{\infty}$ is a sequence which satisfies (4), then

$$y_{2k} = y_{-2} + (k+1)d, \ k \in \mathbf{N}. \tag{8}$$

- If $a = 1$ and $\{y_n\}_{n=-2}^{\infty}$ is a sequence which satisfies (5), then

$$y_{2k+1} = y_{-1} + (k+1)d, \ k \in \mathbf{N}. \tag{9}$$

Therefore, if $b = 0$ in (3), then it reduces to the linear recurrence relation

$$y_n = a y_{n-2} + c, \ n \in \mathbf{N}, \tag{10}$$

and its asymptotic behavior is quite trivial. Indeed, suppose $a \in (0, 1)$. Then any solution $\{y_n\}_{n=-2}^{\infty}$ of (10) satisfies (4) and (5) for $d = c$. Hence by (6) and (7), any solution of (10) tends to $c/(1-a)$. Suppose $a = 1$. Then any solution $\{y_n\}_{n=-2}^{\infty}$ of (10) satisfies (4) and (5) for $d = c$. Hence by (8) and (9), we may see that for any solution $\{y_n\}_{n=-2}^{\infty}$ of (10), $\lim_n y_n = +\infty$ when $c > 0$, $\lim_n y_n = -\infty$ when $c < 0$ while $y_{2n} = y_{-2}$ and $y_{2n+1} = y_{-1}$ for $n \in \mathbf{N}$ when $c = 0$.

Suppose $a > 1$. Then a solution $\{y_n\}_{n=-2}^{\infty}$ of (10) satisfies (4) and (5) for $d = c$. Hence by (6) and (7), we may summarize its limiting behavior in the following table:

Table 1:

y_{-2}	y_{-1}	y_{2n}	y_{2n+1}
$= c/(1-a)$	$= c/(1-a)$	$\to c/(1-a)$	$\to c/(1-a)$
$= c/(1-a)$	$> c/(1-a)$	$\to c/(1-a)$	$\to +\infty$
$> c/(1-a)$	$= c/(1-a)$	$\to +\infty$	$\to c/(1-a)$
$= c/(1-a)$	$< c/(1-a)$	$\to c/(1-a)$	$\to -\infty$
$< c/(1-a)$	$= c/(1-a)$	$\to -\infty$	$\to c/(1-a)$
$> c/(1-a)$	$> c/(1-a)$	$\to +\infty$	$\to +\infty$
$< c/(1-a)$	$< c/(1-a)$	$\to -\infty$	$\to -\infty$
$> c/(1-a)$	$< c/(1-a)$	$\to +\infty$	$\to -\infty$
$< c/(1-a)$	$> c/(1-a)$	$\to -\infty$	$\to +\infty$

For instance, the second row states that if $y_{-2} = y_{-1} = c/(1-a)$, then $y_n \to c/(1-a)$; while the last row states that if $y_{-2} < c/(1-a)$ and $y_{-1} > c/(1-a)$, then $\lim_n y_{2n} = -\infty$ and $\lim_n y_{2n+1} = +\infty$. We remark that the condition $y_{-2} = y_{-1} = c/(1-a)$, as can be seen from (4) and (5), actually implies $y_n = c/(1-a)$ for $n \in \mathbf{N}$. However, in this paper, we only emphasize on limits and hence similar remarks in later discussions will be skipped.

Next, we assume that $b \neq 0$. Then by the transformation $x_n = y_n - \lambda$, we see that (3) is equivalent to

$$x_n = ax_{n-2} + bH(x_{n-1}) + (c + (a-1)\lambda),\ n \in \mathbf{N}, \tag{11}$$

where H is the Heaviside function defined in (1). In particular, if $a = 1$ and $b \neq 0$, then (11) is reduced to

$$x_n = x_{n-2} + bH(x_{n-1}) + c,\ n \in \mathbf{N}. \tag{12}$$

Furthermore, if $a \in (0,1)$ and $b > 0$, or, $a > 1$ and $b < 0$, then by the transformation $z_n = \frac{1-a}{b}x_n$, (11) is equivalent to

$$z_n = az_{n-2} + (1-a)H(z_{n-1}) + d,\ n \in \mathbf{N}; \tag{13}$$

while if $a \in (0,1)$ and $b < 0$, or, $a > 1$ and $b > 0$, then by the same transformation $z_n = \frac{1-a}{b}x_n$, (11) is equivalent to

$$z_n = az_{n-2} + (1-a)G(z_{n-1}) + d,\ n \in \mathbf{N}, \tag{14}$$

where G is the Heaviside function defined in (1) and

$$d = \frac{1-a}{b}(c + (a-1)\lambda).$$

Therefore, we may turn our attention to the equations (12), (13) and (14). Since (14) is similar to (13), we may further turn our attention to the following equation

$$x_n = ax_{n-2} + bH(x_{n-1}) + c,\ n \in \mathbf{N}, \tag{15}$$

which includes (12) and (13) by assuming the cases: (i) $a = 1, b > 0$, (ii) $a = 1, b < 0$, (iii) $a \in (0,1), b > 0$, or (iv) $a > 1, b < 0$.

Henceforth, we will discuss the limiting behaviors of solutions of (15) under the four different sets of conditions on a and b.

To state the corresponding results, it is convenient to introduce some notations. First we set

$$\begin{aligned}
\alpha_{\pm} &= \frac{c \pm b}{1-a}, \\
a^{\pm}_{\eta,k} &= \frac{1}{a^k}\left(\eta - \frac{1-a^k}{1-a}(c \pm b)\right),\ k \in \mathbf{N}, \\
a^{\pm}_{\eta,-k} &= a^k\eta + \frac{1-a^k}{1-a}(c \pm b),\ k \in \mathbf{N}, \\
b^{\pm}_k &= -k(c \pm b),\ k \in \mathbf{N}.
\end{aligned}$$

We will also set

$$a_k^{\pm} = a_{0,k}^{\pm}, a_{-k}^{\pm} = a_{0,-k}^{\pm}, k \in \mathbf{N}.$$

Next, if I and J are real intervals, their cross product $I \times J$ will be denoted by IJ, and we will assume that this product receives the **priority** attention in a mathematical expression. For instance, if we set

$$\mathbf{R}^- = (-\infty, 0], \mathbf{R}^+ = (0, \infty),$$

then $\{\mathbf{R}^+\mathbf{R}^+, \mathbf{R}^+\mathbf{R}^-, \mathbf{R}^-\mathbf{R}^+, \mathbf{R}^-\mathbf{R}^-\}$ is a partition of $\mathbf{R}^2$. Other subsets of the plane will be introduced in the subsequent sections. Here we will employ the following notations

$$a + \Omega = \{a + x |\ x \in \Omega\}$$

and

$$a\Omega = \{ax |\ x \in \Omega\}$$

for any $\Omega \subseteq \mathbf{R}$ and $a \in \mathbf{R}$.

2 The Case where $a = 1$ and $b > 0$

Under the assumption that $a = 1$ and $b > 0$, the limiting behavior of (15) only depends on $c - b$ and $c + b$. Since $c - b < c + b$, we need to consider five cases (i) $0 < c - b$, (ii) $c + b < 0$, (iii) $c + b = 0$, (iv) $c - b = 0$, and (v) $c - b < 0 < c + b$.

Theorem 2.1. Suppose $a = 1, b > 0$ and $0 < c - b$. Then every solution of (15) tends to $+\infty$.

Proof. Let $\{x_k\}_{k=-2}^{\infty}$ be a solution of (15). We first show that exists $m \geq -2$ such that $x_m \in \mathbf{R}^+$. Indeed, suppose to the contrary that $x_k \leq 0$ for all $k \geq -2$. Then $x_k = x_{k-2} + b + c$ for all $k \in \mathbf{N}$. One sees immediately from (8) and (9) $\lim_{n\to\infty} x_n = +\infty$, which is a contradiction.

Next we assert that there exists $m \geq -2$ such that $x_m, x_{m+1} \in \mathbf{R}^+$. Indeed, by the previous discussion, there is $m_0 \geq -2$ such that $x_{m_0} \in \mathbf{R}^+$. If $x_{m_0+1} \in \mathbf{R}^+$, we are done. Otherwise, from

$$x_{m_0+2} = x_{m_0} - b + c > -b + c > 0$$

we have $x_{m_0+2} \in \mathbf{R}^+$. Repeating the argument, we either find $m > m_0$ such that $x_m, x_{m+1} \in \mathbf{R}^+$ or one has that the subsequence x_{m_0+2k} lies in $\mathbf{R}^+$ whereas $x_{m_0+2k+1} \notin \mathbf{R}^+$. This shows that the subsequence $\{x_{m_0+2k+1}\}$ satisfies equation (4) or (5) for $d = -b + c$ and hence $\lim x_{m_0+2k+1} = +\infty > 0$, a contradiction.

Therefore, we may suppose without loss of generality that $x_{-2}, x_{-1} \in \mathbf{R}^+$. Then by (15) and induction, $x_n \in \mathbf{R}^+$ for all $n \geq -2$. Thus $x_n = x_{n-2} - b + c$ for $n \in \mathbf{N}$. In view of (8) and (9), $\lim_{n\to\infty} x_n = +\infty$. The proof is complete.

Theorem 2.2. Suppose $a = 1, b > 0$ and $c + b < 0$. Then every solution of (15) tends to $-\infty$.

The proof is similar to that of Theorem 2.1 and hence skipped.

In the next result, we assume that $a = 1, b > 0$ and $c + b = 0$. Then $0 = b_0^- < b_1^- < \cdots < b_k^- \to +\infty$. If we let

$$C^{(k)} = (b_k^-, b_{k+1}^-], \ k \in \mathbf{N},$$

then

$$C^{(0)} - b + c \subseteq \mathbf{R}^-,$$

$$C^{(k)} - b + c = C^{(k-1)}, \ k \geq 1$$

and

$$\mathbf{R}^+ = \bigcup_{k=0}^{\infty} C^{(k)}.$$

Theorem 2.3. Suppose $a = 1, b > 0$ and $c + b = 0$. Let $\{x_n\}_{n=-2}^{\infty}$ be any solution of (15). Then its limiting behavior can be summarized in the following table:

Table 2:

x_{-2}	x_{-1}	condition	x_{2n}	x_{2n+1}
$\in \mathbf{R}^-$	$\in \mathbf{R}^-$		$\to x_{-2}$	$\to x_{-1}$
$\in \mathbf{R}^+$	$\in \mathbf{R}^-$		$\to x_{-2}$	$\to -\infty$
$\in \mathbf{R}^-$	$\in \mathbf{R}^+$		$\to -\infty$	$\to x_{-1}$
$\in C^{(k)}$	$\in C^{(s)}$	$0 \leq s < k$	$\to x_{2s}$	$\to -\infty$
$\in C^{(k)}$	$\in C^{(s)}$	$0 \leq k \leq s$	$\to -\infty$	$\to x_{2k-1}$

Proof. (i) Suppose $(x_{-2}, x_{-1}) \in \mathbf{R}^-\mathbf{R}^-$. Then from (15) we see that

$$\begin{aligned} x_0 &= x_{-2} + bH(x_{-1}) + c = x_{-2} + b + c = x_{-2} \in \mathbf{R}^-, \\ x_1 &= x_{-1} + bH(x_0) - b = x_{-1} + b + c = x_{-1} \in \mathbf{R}^-. \end{aligned}$$

By induction, one may easily see that $x_{2n} = x_{-2}$ and $x_{2n+1} = x_{-1}$ for all $n \in \mathbf{N}$.

(ii) Suppose $(x_{-2}, x_{-1}) \in \mathbf{R}^+\mathbf{R}^-$. Then by (15),

$$\begin{aligned} x_0 &= x_{-2} + bH(x_{-1}) + c = x_{-2} + b + c = x_{-2} \in \mathbf{R}^+, \\ x_1 &= x_{-1} + bH(x_0) + c = x_{-1} - b + c < x_{-1} \in \mathbf{R}^-. \end{aligned}$$

By induction, $x_{2n} = x_{-2} \in \mathbf{R}^+$ and $x_{2n+1} \in \mathbf{R}^-$ for all $n \in \mathbf{N}$. Furthermore, by (5) and (9) with $d = -b + c = -2b$, $\lim_n x_{2n+1} = -\infty$ as required.

(iii) As in (ii), we may show in similar manners that $(x_{-2}, x_{-1}) \in \mathbf{R}^-\mathbf{R}^+$ implies $\lim x_{2n} = -\infty$ and $\lim x_{2n+1} = x_{-1}$.

(iv) Suppose $(x_{-2}, x_{-1}) \in C^{(k)}C^{(s)}$ where $0 \le s < k$. Then by (15),

$$\begin{aligned} x_0 &= x_{-2} + bH(x_{-1}) + c = x_{-2} - b + c \in C^{(k)} - b + c = C^{(k-1)}, \\ x_1 &= x_{-1} + bH(x_0) + c = x_{-1} - b + c \in C^{(s)} - b + c = C^{(s-1)}, \end{aligned}$$

and by induction, $(x_{2s}, x_{2s+1}) \in \mathbf{R}^+\mathbf{R}^-$. We may proceed as in (ii) to obtain our conclusion.

(v) Suppose $(x_{-2}, x_{-1}) \in C^{(k)}C^{(s)}$ where $0 \le k \le s$. Then by (15), if $k = 0$, then

$$x_0 = x_{-2} + bH(x_{-1}) + c = x_{-2} - b + c \in C^{(0)} - b + c \subseteq \mathbf{R}^-.$$

That is $(x_{-1}, x_0) \in \mathbf{R}^+\mathbf{R}^-$. If $k > 0$, then

$$\begin{aligned} x_0 &= x_{-2} + bH(x_{-1}) + c = x_{-2} - b + c \in C^{(k)} - b + c = C^{(k-1)}, \\ x_1 &= x_{-1} + bH(x_0) + c = ax_{-1} - b + c \in C^{(s)} - b + c = C^{(s-1)}, \end{aligned}$$

and by induction, $(x_{2k-1}, x_{2k}) \in \mathbf{R}^+\mathbf{R}^-$. We may now proceed as in (ii) to obtain our conclusion.

The proof is complete.

In the next result, we assume that $a = 1, b > 0$ and $c - b = 0 < c + b$. Then $0 = b_0^+ > b_1^+ > \cdots > b_k^+ \to -\infty$. If we let

$$D^{(k)} = (b_{k+1}^+, b_k^+],\ k \in \mathbf{N},$$

then

$$D^{(0)} + b + c \subseteq \mathbf{R}^+,$$

$$D^{(k)} + b + c = D^{(k-1)},\ k \ge 1,$$

and

$$\mathbf{R}^- = \bigcup_{k=0}^{\infty} D^{(k)}.$$

By methods similar to the proof of the Theorem 2.3, we may easily obtain the following result.

Theorem 2.4. Suppose $a = 1, b > 0$ and $c - b = 0 < c + b$. Let $\{x_n\}_{n=-2}^{\infty}$ be any solution of (15). Then its limiting behavior can be summarized in the following table:

Table 3:

x_{-2}	x_{-1}	condition	x_{2n}	x_{2n+1}
$\in \mathbf{R}^+$	$\in \mathbf{R}^+$		$\to x_{-2}$	$\to x_{-1}$
$\in \mathbf{R}^-$	$\in \mathbf{R}^+$		$\to x_{-2}$	$\to +\infty$
$\in \mathbf{R}^+$	$\in \mathbf{R}^-$		$\to +\infty$	$\to x_{-1}$
$\in D^{(k)}$	$\in D^{(s)}$	$0 \le s < k$	$\to x_{2s}$	$\to +\infty$
$\in D^{(k)}$	$\in D^{(s)}$	$0 \le k \le s$	$\to +\infty$	$\to x_{2k-1}$

In the next result, we assume that $a = 1, b > 0$ and $c - b < 0 < c + b$. Then $b_0^- < b_1^- < \cdots < b_k^- \to +\infty$ and $b_0^+ > b_1^+ > \cdots > b_k^+ \to -\infty$. We may therefore use the same notations $C^{(k)}$ and $D^{(k)}$ in the previous two cases.

Theorem 2.5. Suppose $a = 1, b > 0$ and $c - b < 0 < c + b$. Let $\{x_n\}_{n=-2}^{\infty}$ be any solution of (15).

(i) If $(x_{-2}, x_{-1}) \in \mathbf{R}^+\mathbf{R}^- \cup C^{(k)}C^{(s)} \cup D^{(r)}D^{(t)}$ where $0 \le s < k$ and $0 \le r \le t$, then $\lim_n x_{2n} = +\infty$ and $\lim_n x_{2n+1} = -\infty$.

(ii) If $(x_{-2}, x_{-1}) \in \mathbf{R}^-\mathbf{R}^+ \cup C^{(k)}C^{(s)} \cup D^{(r)}D^{(t)}$ where $0 \le k \le s$ and $0 \le t < r$, then $\lim_n x_{2n} = -\infty$ and $\lim_n x_{2n+1} = +\infty$.

Proof. (i) Suppose $(x_{-2}, x_{-1}) \in C^{(k)}C^{(s)}$ where $0 \le s < k$. Then by (15),

$$\begin{aligned} x_0 &= x_{-2} + bH(x_{-1}) + c = x_{-2} - b + c \in C^{(k)} - b + c = C^{(k-1)}, \\ x_1 &= x_{-1} + bH(x_0) + c = x_{-1} - b + c \in C^{(s)} - b + c = C^{(s-1)}, \end{aligned}$$

and by induction, $(x_{2s}, x_{2s+1}) \in \mathbf{R}^+\mathbf{R}^-$. Suppose $(x_{-2}, x_{-1}) \in D^{(r)}D^{(t)}$ where $0 \le r \le t$. Then by (15), if $r = 0$, then

$$\begin{aligned} x_0 &= x_{-2} + bH(x_{-1}) + c = x_{-2} + b + c \in D^{(0)} + b + c = D^{(-1)} \subseteq \mathbf{R}^+, \\ x_1 &= x_{-1} + bH(x_0) + c = x_{-1} - b + c < x_{-1} \le 0, \end{aligned}$$

i.e., $(x_0, x_1) \in \mathbf{R}^+\mathbf{R}^-$; while if $r > 0$, then

$$\begin{aligned} x_0 &= x_{-2} + bH(x_{-1}) + c = x_{-2} + b + c \in D^{(r)} - b + c = D^{(r-1)}, \\ x_1 &= ax_{-1} + bH(x_0) + c = x_{-1} + b + c \in D^{(t)} - b + c = D^{(t-1)}, \end{aligned}$$

and by induction, $(x_{2r}, x_{2r+1}) \in \mathbf{R}^+\mathbf{R}^-$.

Therefore, we may suppose without loss of generality that $(x_{-2}, x_{-1}) \in \mathbf{R}^+\mathbf{R}^-$. By (15) and induction, we may then see that $(x_{2n}, x_{2n+1}) \in \mathbf{R}^+\mathbf{R}^-$ for all $n \in \mathbf{N}$. Thus $x_{2n} = x_{2n-2} + b + c$ and $x_{2n+1} = x_{2n-1} - b + c$ for $n \in \mathbf{N}$. In view of (8) and (9), $\lim_{n\to\infty} x_{2n} = +\infty$ and $\lim_{n\to\infty} x_{2n+1} = -\infty$ as desired.

(ii) This case is similar to the case (i) and its proof is skipped.

The proof is complete.

3 The Case where $a = 1$ and $b < 0$

Under the assumption that $a = 1$ and $b < 0$, equation (15) is equivalent to

$$x_n = ax_{n-2} + \widetilde{b}\widetilde{H}(x_{n-1}) + c,\ n \in \mathbf{N},$$

where $\widetilde{b} = -b > 0$ and $\widetilde{H} = -H$. Hence this case is similar to (but not the same as) that where $b > 0$ and $a = 1$. Indeed, under the assumption that $b < 0$ and $a = 1$, the corresponding asymptotic behavior of (15) only depends on $c + b$ and $c - b$. Since $c + b < c - b$, we again have five cases: (i) $c - b < 0$, (ii) $c - b = 0$, (iii) $c + b = 0$, (iv) $c + b < 0 < c - b$, and (v) $c + b > 0$.

The ideas of the proofs of the corresponding asymptotic behaviors are also similar, and hence some of the proofs in this section will be skipped or sketched.

Theorem 3.1. Suppose $a = 1, b < 0$ and $c - b < 0$. Then every solution of (15) tends to $-\infty$.

Theorem 3.2. Suppose $a = 1, b < 0$ and $c + b > 0$. Then every solution of (15) tends to $+\infty$.

Theorem 3.3. Suppose $a = 1, b < 0$ and $c - b = 0$. Let $\{x_n\}_{n=-2}^{\infty}$ be any solution of (15).

(i) If $(x_{-2}, x_{-1}) \in \mathbf{R}^+\mathbf{R}^+$, then $\lim_n x_{2n} = x_{-2}$ and $\lim_n x_{2n+1} = x_{-1}$.

(ii) If $(x_{-2}, x_{-1}) \in \mathbf{R}^+\mathbf{R}^- \cup \mathbf{R}^-\mathbf{R}^+ \cup \mathbf{R}^-\mathbf{R}^-$, then $\lim_n x_n = -\infty$.

Proof. (i) Suppose $(x_{-2}, x_{-1}) \in \mathbf{R}^+\mathbf{R}^+$. Then by (15), $x_0 = x_{-2} - b + c = x_{-2}$, $x_1 = x_{-1} - b + c = x_{-1}$, and by induction, we may easily see that $x_{2n} = x_{-2}$ and $x_{2n+1} = x_{-1}$ for $n \in \mathbf{N}$.

(ii) Suppose $(x_{-2}, x_{-1}) \in \mathbf{R}^+\mathbf{R}^-$. Then $x_{-2} \in (b_k^+, b_{k+1}^+]$ for some $k \in \mathbf{N}$. By (15) and induction, $(x_{2k-1}, x_{2k}) \in \mathbf{R}^-\mathbf{R}^-$. Suppose $(x_{-2}, x_{-1}) \in \mathbf{R}^-\mathbf{R}^+$. Then $x_{-1} \in (b_k^+, b_{k+1}^+]$ for some $k \in \mathbf{N}$. By (15) and induction, $(x_{2k}, x_{2k+1}) \in \mathbf{R}^-\mathbf{R}^-$. Therefore, we may suppose without loss of generality that $(x_{-2}, x_{-1}) \in \mathbf{R}^-\mathbf{R}^-$. Then by (15) and induction, $(x_{2n}, x_{2n+1}) \in \mathbf{R}^-\mathbf{R}^-$ for all $n \geq -2$. Thus $x_n = x_{n-2} + b + c$ for $n \in \mathbf{N}$. In view of (8) and (9), $\lim_{n\to\infty} x_n = -\infty$.

Similar to Theorem 3.3, we may show the Theorem 3.4 as follows.

Theorem 3.4. Suppose $a = 1, b < 0$ and $c + b = 0$. Let $\{x_n\}_{n=-2}^{\infty}$ be any solution of (15).

(i) If $(x_{-2}, x_{-1}) \in \mathbf{R}^-\mathbf{R}^-$, then $\lim_n x_{2n} = x_{-2}$ and $\lim_n x_{2n+1} = x_{-1}$ for all $n \in \mathbf{N}$.

(ii) If $(x_{-2}, x_{-1}) \in \mathbf{R}^+\mathbf{R}^- \cup \mathbf{R}^-\mathbf{R}^+ \cup \mathbf{R}^+\mathbf{R}^+$, then $\lim_n x_n = +\infty$.

In the next result, we assume that $a = 1, b < 0$ and $c + b < 0 < c - b$. Then $b_0^- > b_1^- > \cdots > b_k^- \to -\infty$ and $b_0^+ < b_1^+ < \cdots < b_k^+ \to +\infty$. Let

$$\overline{C}^{(k)} = (b_{k+1}^-, b_k^-], \overline{D}^{(k)} = (b_k^+, b_{k+1}^+]$$

for $k \in \mathbf{N}$, then

$$\mathbf{R}^- = \bigcup_{k=0}^{\infty} \overline{C}^{(k)}, \mathbf{R}^+ = \bigcup_{k=0}^{\infty} \overline{D}^{(k)}.$$

Theorem 3.5. Suppose $a = 1, b < 0, c + b < 0 < c - b$. Let $\{x_n\}_{n=-2}^{\infty}$ be any solution of (15).

(i) If $(x_{-2}, x_{-1}) \in \overline{C}^{(k)}\overline{D}^{(s)} \cup \overline{D}^{(r)}\overline{C}^{(t)} \cup \mathbf{R}^-\mathbf{R}^-$ where $0 \le s < k$ and $0 \le r \le t$, then $\lim_n x_n = -\infty$.

(ii) If $(x_{-2}, x_{-1}) \in \overline{C}^{(k)}\overline{D}^{(s)} \cup \overline{D}^{(r)}\overline{C}^{(t)} \cup \mathbf{R}^+\mathbf{R}^+$ where $0 \le k \le s$ and $0 \le t < r$, then $\lim_n x_n = +\infty$.

Proof. (i) Suppose$(x_{-2}, x_{-1}) \in \overline{C}^{(k)}\overline{D}^{(s)}$ where $0 \le s < k$. Then as in the proof of Theorem 2.5, by (15) and induction, $(x_{2s}, x_{2s+1}) \in \mathbf{R}^-\mathbf{R}^-$. Suppose $(x_{-2}, x_{-1}) \in \overline{D}^{(r)}\overline{C}^{(t)}$ where $0 \le r \le t$. Then by (15) and induction, $(x_{2r-1}, x_{2r}) \in \mathbf{R}^-\mathbf{R}^-$. Therefore, we may suppose without loss of generality that $(x_{-2}, x_{-1}) \in \mathbf{R}^-\mathbf{R}^-$. Then by (15) and induction, $(x_{2n}, x_{2n+1}) \in \mathbf{R}^-\mathbf{R}^-$ for all $n \ge -2$. Thus $x_n = x_{n-2} + b + c$ for $n \in \mathbf{N}$. In view of (8) and (9), $\lim_{n\to\infty} x_n = -\infty$.

(ii) This case is similar to the previous case (i) and its proof is skipped. where $\widetilde{b} = -b > 0$ and $\widetilde{H} = -H$. Hence this case is similar to (but not the same as) that where $b > 0$ and $a = 1$. Indeed, under the assumption that $b < 0$ and $a = 1$, the corresponding asymptotic behavior of (15) only depends on $c + b$ and $c - b$. Since $c + b < c - b$, we again have five cases: (i) $c - b < 0$, (ii) $c - b = 0$, (iii) $c + b = 0$, (iv) $c + b < 0 < c - b$, and (v) $c + b > 0$.

The ideas of the proofs of the corresponding asymptotic behaviors are also similar, and hence some of the proofs in this section will be skipped or sketched.

4 The Case where $a \in (0,1)$ and $b > 0$

Under the assumption that $a \in (0,1)$, we have $\alpha_- = (c-b)/(1-a) < (c+b)/(1-a) = \alpha_+$. Thus we need to consider five cases (i) $0 < \alpha_-$, (ii) $0 = \alpha_-$, (iii) $\alpha_- < 0 < \alpha_+$, (iv) $0 = \alpha_+$, and (v) $0 > \alpha_+$.

Theorem 4.1. Suppose $a \in (0,1), b > 0$ and $\alpha_+ < 0$. Then every solution of (15) tends to α_+.

Proof. Let $\{x_k\}_{k=-2}^{\infty}$ be a solution of (15). If $x_k > 0$ for all $k \geq -2$, then from (15), $x_k = ax_{k-2} - b + c$ for all $k \in \mathbf{N}$. One sees immediately from (6) and (7) that $\lim_n x_n = (c-b)/(1-a) = \alpha_- < \alpha_+ < 0$, which is a contradiction. Thus there is $m \geq -2$ such that $x_m \in \mathbf{R}^-$. Then we may show as in the proof of Theorem 2.1 that there exists $m \geq -2$ such that $x_m, x_{m+1} \in \mathbf{R}^-$. Therefore, we may suppose without loss of generality that $x_{-2}, x_{-1} \in \mathbf{R}^-$. Then by (15) and induction, $x_n \in \mathbf{R}^-$ for all $n \geq -2$. Thus $x_n = ax_{n-2} + b + c$ for $n \in \mathbf{N}$. In view of (6) and (7), $\lim_{n\to\infty} x_n = \alpha_+$. The proof is complete.

Theorem 4.2. Suppose $a \in (0,1), b > 0$ and $\alpha_- > 0$. Then every solution of (15) tends to α_-.

The proof is similar to that of Theorem 4.1 and hence is omitted.

In the next result, we assume that $a \in (0,1), b > 0$ and $\alpha_+ = 0$. Then $0 = a_0^- < a_1^- < \cdots < a_k^- \to +\infty$. If we let

$$A^{(k)} = (a_k^-, a_{k+1}^-],\ k \in \mathbf{N},$$

and

$$A^{(-1)} = aA^{(0)} - b + c = (-b + c, 0],$$

then

$$A^{(k-1)} = aA^{(k)} - b + c,\ k \in \mathbf{N},$$

$$A^{(-1)} \subseteq \mathbf{R}^-,$$

and

$$\mathbf{R}^+ = \bigcup_{k=0}^{\infty} A^{(k)}.$$

Theorem 4.3. Suppose $a \in (0,1), b > 0$ and $0 = \alpha_+$. Let $\{x_n\}_{n=-2}^{\infty}$ be any solution of (15).

(i) If $(x_{-2}, x_{-1}) \in \mathbf{R}^-\mathbf{R}^-$, then $\lim_n x_n = 0$.

(ii) If $(x_{-2}, x_{-1}) \in A^{(k)}A^{(s)} \cup \mathbf{R}^+\mathbf{R}^-$ where $0 \le s < k$, then $\lim_n x_{2n} = 0$ and $\lim_n x_{2n+1} = \alpha_-$.

(iii) If $(x_{-2}, x_{-1}) \in A^{(k)}A^{(s)} \cup \mathbf{R}^-\mathbf{R}^+$ where $0 \le k \le s$, then $\lim_n x_{2n} = \alpha_-$ and $\lim_n x_{2n+1} = 0$.

Proof. The proof of (i) is quite easy in view of the proofs of Theorems 2.3, 2.4 and 2.5, and hence skipped. To see (ii), suppose $(x_{-2}, x_{-1}) \in A^{(k)}A^{(s)}$ where $0 \le s < k$. Then by (15),

$$\begin{aligned} x_0 &= ax_{-2} + bH(x_{-1}) + c = ax_{-2} - b + c \in aA^{(k)} - b + c = A^{(k-1)}, \\ x_1 &= ax_{-1} + bH(x_0) + c = ax_{-1} - b + c \in aA^{(s)} - b + c = A^{(s-1)}, \end{aligned}$$

and by induction, $(x_{2s}, x_{2s+1}) \in A^{(k-s-1)}A^{(-1)} \subseteq \mathbf{R}^+\mathbf{R}^-$. Therefore, we may suppose without loss of generality $(x_{-2}, x_{-1}) \in \mathbf{R}^+\mathbf{R}^-$. Then by (15) and induction, $(x_{2n}, x_{2n+1}) \in \mathbf{R}^+\mathbf{R}^-$ for all $n \ge -2$. Thus $x_{2n} = ax_{2n-2} + b + c$ and $x_{2n+1} = ax_{2n-1} - b + c$. In view of (6) and (7), $\lim_{n\to\infty} x_{2n} = 0$ and $\lim_{n\to\infty} x_{2n+1} = \alpha_-$ as desired. Finally, the proof of (iii) is similar to that of the case (ii) and hence omitted.

In the next result, we assume that $a \in (0,1), b > 0$ and $\alpha_- = 0$. Then $0 = a_0^+ > a_1^+ > \cdots > a_k^+ \to -\infty$ and $(-\infty, 0) = \bigcup_{k=0}^{\infty}[a_{k+1}^+, a_k^+)$.

Theorem 4.4. Suppose $a \in (0,1), b > 0$ and $\alpha_- = 0$. Let $\{x_n\}_{n=-2}^{\infty}$ be any solution of (15). Then its limiting behavior can be summarized in the following table:

Table 4:

x_{-2}	x_{-1}	condition	x_{2n}	x_{2n+1}
$\in \mathbf{R}^+$	$\in \mathbf{R}^+$		$\to 0$	$\to 0$
$\in (a_1^+, +\infty)$	$= 0$		$\to \alpha_+$	$\to 0$
$\in \mathbf{R}^-$	$\in \mathbf{R}^+$		$\to 0$	$\to \alpha_+$
$\in (-\infty, a_1^+]$	$= 0$		$\to 0$	$\to \alpha_+$
$\in [0, +\infty)$	$\in (-\infty, 0)$		$\to \alpha_+$	$\to 0$
$\in [a_{k+1}^+, a_k^+)$	$\in [a_{s+1}^+, a_s^+)$	$0 \le k < s$	$\to \alpha_+$	$\to 0$
$\in [a_{k+1}^+, a_k^+)$	$= a_{s+1}^+$	$0 \le k = s$	$\to \alpha_+$	$\to 0$
$= a_{k+1}^+$	$\in (a_{s+1}^+, a_s^+)$	$0 \le k = s$	$\to 0$	$\to \alpha_+$
$\in (a_{k+1}^+, a_k^+)$	$\in (a_{s+1}^+, a_s^+)$	$0 \le k = s$	$\to \alpha_+$	$\to 0$
$= a_{k+1}^+$	$\in [a_{s+1}^+, a_s^+)$	$0 \le k = s+1$	$\to 0$	$\to \alpha_+$
$\in (a_{k+1}^+, a_k^+)$	$= a_{s+1}^+$	$0 \le k = s+1$	$\to \alpha_+$	$\to 0$
$\in (a_{k+1}^+, a_k^+)$	$\in (a_{s+1}^+, a_s^+)$	$0 \le k = s+1$	$\to 0$	$\to \alpha_+$
$\in [a_{k+1}^+, a_k^+)$	$\in [a_{s+1}^+, a_s^+)$	$k > s+1$	$\to 0$	$\to \alpha_+$

Again the proof of Theorem 4.4 is similar to those of Theorems 2.3, 2.4 and 2.5, and hence skipped.

In the next result, we assume that $a \in (0,1), b > 0$ and $\alpha_- < 0 < \alpha_+$. Then $0 = a_0^- < a_1^- < \cdots < a_k^- \to +\infty$ and $0 = a_0^+ > a_1^+ > \cdots > a_k^+ \to -\infty$. Therefore, if let $A^{(k)} = (a_k^-, a_{k+1}^-]$ and $B^{(k)} = (a_{k+1}^+, a_k^+]$ for $k \in \mathbf{N}$ and $A^{(-1)} = aA^{(0)} - b + c$ and $B^{(-1)} = aB^{(0)} + b + c$, then

$$aA^{(k)} - b + c = A^{(k-1)}, aB^{(k)} + b + c = B^{(k-1)}, k \in \mathbf{N},$$

$$A^{(-1)} \subseteq \mathbf{R}^-, B^{(-1)} \subseteq \mathbf{R}^+,$$

and

$$\mathbf{R}^+ = \bigcup_{k=0}^{\infty} A^{(k)},\ \mathbf{R}^- = \bigcup_{k=0}^{\infty} B^{(k)}.$$

Theorem 4.5. Suppose $a \in (0,1), b > 0$ and $\alpha_- < 0 < \alpha_+$. Let $\{x_n\}_{n=-2}^{\infty}$ be any solution of (15).

(i) If $(x_{-2}, x_{-1}) \in A^{(k)}A^{(s)} \cup B^{(r)}B^{(t)} \cup \mathbf{R}^+\mathbf{R}^-$ where $0 \le s < k$ and $0 \le r \le t$, then $\lim_n x_{2n} = \alpha_+$ and $\lim_n x_{2n+1} = \alpha_-$.

(ii) If $(x_{-2}, x_{-1}) \in A^{(k)}A^{(s)} \cup B^{(r)}B^{(t)} \cup \mathbf{R}^-\mathbf{R}^+$ where $0 \le k \le s$ and $0 \le t < r$, then $\lim_n x_{2n} = \alpha_-$ and $\lim_n x_{2n+1} = \alpha_+$.

Proof. Suppose $(x_{-2}, x_{-1}) \in A^{(k)}A^{(s)}$ where $0 \le s < k$. Then by (15),

$$\begin{aligned} x_0 &= ax_{-2} + bH(x_{-1}) + c = ax_{-2} - b + c \in aA^{(k)} - b + c = A^{(k-1)}, \\ x_1 &= ax_{-1} + bH(x_0) + c = ax_{-1} - b + c \in aA^{(s)} - b + c = A^{(s-1)}, \end{aligned}$$

and by induction, $(x_{2s}, x_{2s+1}) \in A^{(k-s-1)}A^{(-1)} \subseteq \mathbf{R}^+\mathbf{R}^-$. Suppose $(x_{-2}, x_{-1}) \in B^{(r)}B^{(t)}$ where $0 \le r \le t$. By (15), if $r = 0$, then

$$\begin{aligned} x_0 &= ax_{-2} + bH(x_{-1}) + c = ax_{-2} + b + c \in aB^{(0)} + b + c = B^{(-1)} \subseteq \mathbf{R}^+, \\ x_1 &= ax_{-1} + bH(x_0) + c = ax_{-1} - b + c \le -b + c < 0, \end{aligned}$$

i.e., $(x_0, x_1) \in \mathbf{R}^+\mathbf{R}^-$; while if $r > 0$, then

$$\begin{aligned} x_0 &= ax_{-2} + bH(x_{-1}) + c = ax_{-2} + b + c \in aB^{(r)} + b + c = B^{(r-1)}, \\ x_1 &= ax_{-1} + bH(x_0) + c = ax_{-1} + b + c \in aB^{(t)} + b + c = B^{(t-1)}, \end{aligned}$$

and by induction,$(x_{2r}, x_{2r+1}) \in \mathbf{R}^+\mathbf{R}^-$. Therefore, we may suppose without loss of generality that $(x_{-2}, x_{-1}) \in \mathbf{R}^+\mathbf{R}^-$. Then by (15) and induction, $(x_{2n}, x_{2n+1}) \in \mathbf{R}^+\mathbf{R}^-$ for all $n \ge -2$. Thus $x_{2n} = ax_{2n-2} + b + c$ and $x_{2n+1} = ax_{2n-1} - b + c$ for $n \in \mathbf{N}$. In view of (6) and (7), $\lim_{n\to\infty} x_{2n} = \alpha_+$ and $\lim_{n\to\infty} x_{2n+1} = \alpha_-$ as desired.

The conclusion (ii) is similar to (i) and its proof is omitted.

5 The Case where $a > 1$ and $b < 0$

Under the assumption that $a > 1$ and $b < 0$, we have $\alpha_- = (c-b)/(1-a) < (c+b)/(1-a) = \alpha_+$. We therefore need to consider five cases: (i) $\alpha_+ < 0$, (ii) $0 = \alpha_+$,(iii) $\alpha_- < 0 < \alpha_+$, (iv) $0 = \alpha_-$, and (v) $0 < \alpha_-$. Again, the conclusions below are quite similar to those above and their proofs are skipped.

Suppose $a > 1, b < 0$ and $\alpha_+ < 0$. Then $0 = a_0^+ > a_1^+ > \cdots > a_k^+ \longrightarrow \alpha_+$, $\alpha_- = a_{\alpha_-,0}^+ < a_{\alpha_-,1}^+ < \cdots < a_{\alpha_-,k}^+ \longrightarrow \alpha_+$, $\alpha_+ = a_{\alpha_+,0}^- > a_{\alpha_+,1}^- > \cdots > a_{\alpha_+,k}^- \longrightarrow \alpha_-$ and

$$(\alpha_+, 0) = \bigcup_{k=0}^{\infty} [a_{k+1}^+, a_k^+), (\alpha_-, \alpha_+) = \bigcup_{k=0}^{\infty} (a_{\alpha_-,k}^+, a_{\alpha_-,k+1}^+] = \bigcup_{k=0}^{\infty} [a_{\alpha_+,k+1}^-, a_{\alpha_+,k}^-).$$

Theorem 5.1. Suppose $a > 1, b < 0$ and $\alpha_+ < 0$. Let $\{x_n\}_{n=-2}^{\infty}$ be any solution of (15). Then its limiting behaviors can be summarized in the following tables 5 and 6.

Table 5 ($(x_{-2}, x_{-1}) \in \mathbf{R}^2 \backslash \{(\alpha_+, 0) \times (\alpha_-, \alpha_+) \cup (\alpha_-, \alpha_+) \times (\alpha_+, 0)\}$) :

x_{-2}	x_{-1}	x_{2n}	x_{2n+1}
$\in (-\infty, \alpha_+)$	$\in (-\infty, \alpha_+)$	$\to -\infty$	$\to -\infty$
$= \alpha_+$	$\in (-\infty, \alpha_+)$	$\to \alpha_+$	$\to -\infty$
$\in (-\infty, \alpha_+)$	$= \alpha_+$	$\to -\infty$	$\to \alpha_+$
$= \alpha_+$	$= \alpha_+$	$\to \alpha_+$	$\to \alpha_+$
$\in (\alpha_+, +\infty)$	$\in (\alpha_+, +\infty)$	$\to +\infty$	$\to +\infty$
$\in (\alpha_+, +\infty)$	$= \alpha_+$	$\to +\infty$	$\to +\infty$
$= \alpha_+$	$\in (\alpha_+, +\infty)$	$\to +\infty$	$\to +\infty$
$\in [0, +\infty)$	$\in (\alpha_-, \alpha_+)$	$\to +\infty$	$\to +\infty$
$\in (\alpha_-, \alpha_+)$	$\in \mathbf{R}^+$	$\to +\infty$	$\to +\infty$
$\in (a_{\alpha_-,1}^+, \alpha_+]$	$= 0$	$\to +\infty$	$\to +\infty$
$\in (\alpha_+, +\infty)$	$\in (-\infty, \alpha_-)$	$\to +\infty$	$\to -\infty$
$\in (\alpha_+, a_1^+]$	$= \alpha_-$	$\to +\infty$	$\to -\infty$
$\in (-\infty, \alpha_-)$	$\in (\alpha_+, +\infty)$	$\to -\infty$	$\to +\infty$
$= \alpha_-$	$\in (\alpha_+, 0]$	$\to -\infty$	$\to +\infty$
$\in (\alpha_-, a_{\alpha_-,1}^+)$	$= 0$	$\to -\infty$	$\to +\infty$
$\in (a_1^+, +\infty)$	$= \alpha_-$	$\to +\infty$	$\to \alpha_-$
$= \alpha_-$	$\in \mathbf{R}^+$	$\to \alpha_-$	$\to +\infty$
$= a_{\alpha_-,1}^+$	$= 0$	$\to \alpha_-$	$\to +\infty$

Table 6 ($(x_{-2}, x_{-1}) \in (\alpha_+, 0) \times (\alpha_-, \alpha_+) \cup (\alpha_-, \alpha_+) \times (\alpha_+, 0)$):

x_{-2}	x_{-1}	condition	x_{2n}	x_{2n+1}
$\in [a^+_{k+1}, a^+_k)$	$\in (a^+_{\alpha_-,s}, a^+_{\alpha_-,s+1}]$	$k < s$	$\to +\infty$	$\to +\infty$
$\in (a^+_{k+1}, a^+_k)$	$\in (a^+_{\alpha_-,s}, a^+_{\alpha_-,s+1}]$	$k = s$	$\to +\infty$	$\to +\infty$
$= a^+_{k+1}$	$\in (a^+_{\alpha_-,s}, a^+_{\alpha_-,s+1})$	$k = s$	$\to +\infty$	$\to -\infty$
$= a^+_{k+1}$	$= a^+_{\alpha_-,s+1}$	$k = s$	$\to +\infty$	$\to \alpha_-$
$\in [a^+_{k+1}, a^+_k)$	$\in (a^+_{\alpha_-,s}, a^+_{\alpha_-,s+1})$	$k = s+1$	$\to +\infty$	$\to -\infty$
$\in (a^+_{k+1}, a^+_k)$	$= a^+_{\alpha_-,s+1}$	$k = s+1$	$\to +\infty$	$\to \alpha_-$
$= a^+_{k+1}$	$= a^+_{\alpha_-,s+1}$	$k = s+1$	$\to +\infty$	$\to -\infty$
$\in [a^+_{k+1}, a^+_k)$	$\in (a^+_{\alpha_-,s}, a^+_{\alpha_-,s+1}]$	$k > s+1$	$\to +\infty$	$\to -\infty$
$\in (a^+_{\alpha_-,k}, a^+_{\alpha_-,k+1}]$	$\in [a^+_{s+1}, a^+_s)$	$k < s$	$\to -\infty$	$\to +\infty$
$\in (a^+_{\alpha_-,k}, a^+_{\alpha_-,k+1})$	$\in [a^+_{s+1}, a^+_s)$	$k = s$	$\to -\infty$	$\to +\infty$
$= a^+_{\alpha_-,k+1}$	$\in (a^+_{s+1}, a^+_s)$	$k = s$	$\to \alpha_-$	$\to +\infty$
$= a^+_{\alpha_-,k+1}$	$= a^+_{s+1}$	$k = s$	$\to -\infty$	$\to +\infty$
$\in (a^+_{\alpha_-,k}, a^+_{\alpha_-,k+1}]$	$\in (a^+_{s+1}, a^+_s)$	$k = s+1$	$\to +\infty$	$\to +\infty$
$\in (a^+_{\alpha_-,k}, a^+_{\alpha_-,k+1})$	$= a^+_{s+1}$	$k = s+1$	$\to -\infty$	$\to +\infty$
$= a^+_{\alpha_-,k+1}$	$= a^+_{s+1}$	$k = s+1$	$\to \alpha_-$	$\to +\infty$
$\in (a^+_{\alpha_-,k}, a^+_{\alpha_-,k+1}]$	$\in [a^+_{s+1}, a^+_s)$	$k > s+1$	$\to +\infty$	$\to +\infty$

Table 7:

x_{-2}	x_{-1}	x_{2n}	x_{2n+1}
$\in (-\infty, 0)$	$\in (-\infty, 0)$	$\to -\infty$	$\to -\infty$
$\in (-\infty, 0)$	$= 0$	$\to -\infty$	$\to 0$
$= 0$	$\in (-\infty, 0)$	$\to 0$	$\to -\infty$
$= 0$	$= 0$	$\to 0$	$\to 0$
$\in \mathbf{R}^+$	$\in R^+$	$\to +\infty$	$\to +\infty$
$\in \mathbf{R}^+$	$= 0$	$\to +\infty$	$\to +\infty$
$= 0$	$\in \mathbf{R}^+$	$\to +\infty$	$\to +\infty$
$\in \mathbf{R}^+$	$\in (\alpha_-, 0)$	$\to +\infty$	$\to +\infty$
$\in (\alpha_-, 0)$	$\in \mathbf{R}^+$	$\to +\infty$	$\to +\infty$
$\in \mathbf{R}^+$	$\in (-\infty, \alpha_-)$	$\to +\infty$	$\to -\infty$
$\in \mathbf{R}^+$	$= \alpha_-$	$\to +\infty$	$\to \alpha_-$
$\in (-\infty, \alpha_-)$	$\in \mathbf{R}^+$	$\to -\infty$	$\to +\infty$
$= \alpha_-$	$\in \mathbf{R}^+$	$\to \alpha_-$	$\to +\infty$

In the next result, we assume that $a > 1, b < 0$ and $\alpha_- < \alpha_+ = 0$. Then $a^-_{\alpha_+,0} > a^-_{\alpha_+,1} > \cdots > a^-_{\alpha_+,k} \to \alpha_-$ and

$$(\alpha_-, 0) = \bigcup_{k=0}^{\infty} [a^-_{\alpha_+,k+1}, a^-_{\alpha_+,k}).$$

Theorem 5.2. Suppose $a > 1, b < 0$ and $\alpha_+ = 0$. Let $\{x_n\}_{n=-2}^{\infty}$ be any solution of (15). Then its limiting behaviors can be summarized in the above table 7.

In the next result, we assume that $a > 1, b < 0$ and $\alpha_- < 0 < \alpha_+$. Then $0 = a_0^+ < a_1^+ < \cdots < a_k^+ \to \alpha_+$ and $0 = a_0^- > a_1^- > \cdots > a_k^- \to \alpha_-$. Let

$$G^{(k)} = (a_k^+, a_{k+1}^+],\ H^{(k)} = [a_{k+1}^-, a_k^-)$$

for $k \in \mathbf{N}$, then

$$(0, \alpha_+) = \bigcup_{k=0}^{\infty} G^{(k)}, (\alpha_-, 0) = \bigcup_{k=0}^{\infty} H^{(k)}.$$

Theorem 5.3. Suppose $a > 1, b < 0$ and $\alpha_- < 0 < \alpha_+$. Let $\{x_n\}_{n=-2}^{\infty}$ be any solution of (15). Then its limiting behaviors can be summarized in the following tables 8 and 9.

Table 8 ($(x_{-2}, x_{-1}) \in [\alpha_+, +\infty) \times (-\infty, \alpha_-] \cup (-\infty, \alpha_-] \times [\alpha_+, +\infty)$):

x_{-2}	x_{-1}	x_{2n}	x_{2n+1}
$(\alpha_+, +\infty)$	$(-\infty, \alpha_-)$	$\to +\infty$	$\to -\infty$
α_+	$(-\infty, \alpha_-)$	$\to \alpha_+$	$\to -\infty$
$(\alpha_+, +\infty)$	α_-	$\to +\infty$	$\to \alpha_-$
α_+	α_-	$\to \alpha_+$	$\to \alpha_-$
$(-\infty, \alpha_-)$	$(\alpha_+, +\infty)$	$\to -\infty$	$\to +\infty$
$(-\infty, \alpha_-)$	α_+	$\to -\infty$	$\to \alpha_+$
α_-	$(\alpha_+, +\infty)$	$\to \alpha_-$	$\to +\infty$
α_-	α_+	$\to \alpha_-$	$\to \alpha_+$

Table 9 ($(x_{-2}, x_{-1}) \in \mathbf{R}^2 \backslash \{[\alpha_+, +\infty) \times (-\infty, \alpha_-] \cup (-\infty, \alpha_-] \times [\alpha_+, +\infty)\}$):

x_{-2}	x_{-1}	condition	x_{2n}	x_{2n+1}
$\mathbf{R}^-$	$\mathbf{R}^-$		$\to -\infty$	$\to -\infty$
$(-\infty, \alpha_-]$	$(0, \alpha_+)$		$\to -\infty$	$\to -\infty$
$(0, \alpha_+)$	$(-\infty, \alpha_-]$		$\to -\infty$	$\to -\infty$
$(0, a_1^+]$	0		$\to -\infty$	$\to -\infty$
$G^{(k)}$	$H^{(s)}$	$k \le s$	$\to -\infty$	$\to -\infty$
$H^{(r)}$	$G^{(t)}$	$t < r$	$\to -\infty$	$\to -\infty$
$\mathbf{R}^+$	$\mathbf{R}^+$		$\to +\infty$	$\to +\infty$
$[\alpha_+, +\infty)$	$(\alpha_-, 0)$		$\to +\infty$	$\to +\infty$
$(\alpha_-, 0)$	$[\alpha_+, +\infty)$		$\to +\infty$	$\to +\infty$
0	$\mathbf{R}^+$		$\to +\infty$	$\to +\infty$
$(a_1^+, +\infty)$	0		$\to +\infty$	$\to +\infty$
$G^{(k)}$	$H^{(s)}$	$s < k$	$\to +\infty$	$\to +\infty$
$H^{(r)}$	$G^{(t)}$	$r \le t$	$\to +\infty$	$\to +\infty$

Table 10:

x_{-2}	x_{-1}	x_{2n}	x_{2n+1}
$\in \mathbf{R}^+$	$\in \mathbf{R}^+$	$\to +\infty$	$\to +\infty$
$\in \mathbf{R}^-$	$\in \mathbf{R}^-$	$\to -\infty$	$\to -\infty$
$\in (0, \alpha_+)$	$\in \mathbf{R}^-$	$\to -\infty$	$\to -\infty$
$\in \mathbf{R}^-$	$\in (0, \alpha_+)$	$\to -\infty$	$\to -\infty$
$\in (\alpha_+, +\infty)$	$\in (-\infty, 0)$	$\to +\infty$	$\to -\infty$
$\in (-\infty, 0)$	$\in (\alpha_+, +\infty)$	$\to -\infty$	$\to +\infty$
$= \alpha_+$	$\in (-\infty, 0)$	$\to \alpha_+$	$\to -\infty$
$\in (-\infty, 0)$	$= \alpha_+$	$\to -\infty$	$\to \alpha_+$
$\in (\alpha_+, +\infty)$	$= 0$	$\to +\infty$	$\to 0$
$= 0$	$\in (\alpha_+, +\infty)$	$\to 0$	$\to +\infty$
$= 0$	$= \alpha_+$	$\to 0$	$\to \alpha_+$
$= \alpha_+$	$= 0$	$\to \alpha_+$	$\to 0$

In the next result, we assume that $a > 1, b < 0$ and $\alpha_- = 0$. Then $0 = a_0^+ < a_1^+ < \cdots < a_k^+ \to \alpha_+$ and

$$(0, \alpha_+) = \bigcup_{k=0}^{\infty} (a_k^+, a_{k+1}^+].$$

Theorem 5.4. Suppose $a > 1, b < 0$ and $0 = \alpha_-$. Let $\{x_n\}_{n=-2}^{\infty}$ be any solution of (15). Then its limiting behaviors can be summarized in the above table 10.

In the next result, we assume that $a > 1, b < 0$ and $0 < \alpha_-$. Then $0 = a_0^- < a_1^- < \cdots < a_k^- \to \alpha_-$, $\alpha_- = a_{\alpha-,0}^+ < a_{\alpha-,1}^+ < \cdots < a_{\alpha-,k}^+ \longrightarrow \alpha_+$, $\alpha_+ = a_{\alpha+,0}^- > a_{\alpha+,1}^- > \cdots > a_{\alpha+,k}^- \longrightarrow \alpha_-$ and

$$(0, \alpha_-) = \bigcup_{k=0}^{\infty} (a_k^-, a_{k+1}^-], \ (\alpha_-, \alpha_+) = \bigcup_{k=0}^{\infty} (a_{\alpha-,k}^+, a_{\alpha-,k+1}^+] = \bigcup_{k=0}^{\infty} [a_{\alpha+,k+1}^-, a_{\alpha+,k}^-).$$

We also need to break up R^2 into six different parts: (a) $\Gamma_1 = [\alpha_-, \infty)^2$, (b) $\Gamma_2 = [\alpha_+, \infty) \times (-\infty, \alpha_-)$, (c) $\Gamma_3 = (-\infty, \alpha_-) \times [\alpha_+, \infty)$, (d) $\Gamma_4 = (0, \alpha_-) \times (\alpha_-, \alpha_+)$, (e) $\Gamma_5 = (\alpha_-, \alpha_+) \times (0, \alpha_-)$, and (f) $\Gamma_6 = \mathbf{R}^2 \backslash \bigcup_{i=1}^{5} \Gamma_i$.

Theorem 5.5. Suppose $a > 1, b < 0$ where $0 < \alpha_-$. Let $\{x_n\}_{n=-2}^{\infty}$ be any solution of (15). Then $\lim_n x_n = -\infty$ if $(x_{-2}, x_{-1}) \in \Gamma_6$, else its limiting behaviors can be summarized in the following table:

Table 11 ($(x_{-2}, x_{-1}) \in \bigcup_{i=1}^{5} \Gamma_i$):

x_{-2}	x_{-1}	condition	x_{2n}	x_{2n+1}
$(\alpha_-, +\infty)$	$(\alpha_-, +\infty)$		$\to +\infty$	$\to +\infty$
α_-	$(\alpha_-, +\infty)$		$\to \alpha_-$	$\to +\infty$
$(\alpha_-, +\infty)$	α_-		$\to +\infty$	$\to \alpha_-$
α_-	α_-		$\to \alpha_-$	$\to \alpha_-$
$(\alpha_+, +\infty)$	$(-\infty, \alpha_-)$		$\to +\infty$	$\to -\infty$
α_+	$(0, \alpha_-)$		$\to +\infty$	$\to -\infty$
α_+	R^-		$\to \alpha_+$	$\to -\infty$
$(-\infty, \alpha_-)$	$(\alpha_+, +\infty)$		$\to -\infty$	$\to +\infty$
(a_1^-, α_-)	α_+		$\to -\infty$	$\to +\infty$
$(-\infty, a_1^-]$	α_+		$\to -\infty$	$\to \alpha_+$
$(a_k^-, a_{k+1}^-]$	$[a_{\alpha_+,s+1}^-, a_{\alpha_+,s}^-)$	$0 \le k \le s$	$\to -\infty$	$-\infty$
$(a_k^-, a_{k+1}^-]$	$a_{\alpha_+,s+1}^-$	$k = s+1$	$\to -\infty$	$\to \alpha_+$
$(a_k^-, a_{k+1}^-]$	$(a_{\alpha_+,s+1}^-, a_{\alpha_+,s}^-)$	$k = s+1$	$\to -\infty$	$\to +\infty$
$(a_k^-, a_{k+1}^-]$	$[a_{\alpha_+,s+1}^-, a_{\alpha_+,s}^-)$	$k > s+1$	$\to -\infty$	$\to +\infty$
$[a_{\alpha_+,k+1}^-, a_{\alpha_+,k}^-)$	$(a_s^-, a_{s+1}^-]$	$0 \le s < k$	$\to -\infty$	$\to -\infty$
$a_{\alpha_+,k+1}^-$	$(a_s^-, a_{s+1}^-]$	$k = s$	$\to \alpha_+$	$\to -\infty$
$(a_{\alpha_+,k+1}^-, a_{\alpha_+,k}^-)$	$(a_s^-, a_{s+1}^-]$	$k = s$	$\to +\infty$	$\to -\infty$
$[a_{\alpha_+,k+1}^-, a_{\alpha_+,k}^-)$	$(a_s^-, a_{s+1}^-]$	$k < s$	$\to +\infty$	$\to -\infty$

6 Concluding Remarks

Since we have derived the exact relations between the initial pair (x_{-2}, x_{-1}) with the limiting behaviors of the solution $\{x_k\}_{k=-2}^{\infty}$ of (15) originated from it, we may make some interesting observations. For instance,

- in case $a = 1$ and $b > 0$, a solution $\{x_k\}_{k=-2}^{\infty}$ of (15) converges if, and only if, $c + b = 0$ and $x_{-2} = x_{-1} \in \mathbf{R}^-$, or, $c - b = 0$ and $x_{-2} = x_{-1} \in \mathbf{R}^+$;

- in case $a = 1$ and $b < 0$, a solution $\{x_k\}_{k=-2}^{\infty}$ of (15) converges if, and only if, $c - b = 0$ and $x_{-2} = x_{-1} \in \mathbf{R}^+$, or, $c + b = 0$ and $x_{-2} = x_{-1} \in \mathbf{R}^-$;

- in case $a \in (0, 1)$ and $b > 0$, a solution $\{x_k\}_{k=-2}^{\infty}$ of (15) converges if, and only if, (i) $\alpha_+ < 0$, (ii) $\alpha_- > 0$, (iii) $\alpha_+ = 0$ and $x_{-2}, x_{-1} \in \mathbf{R}^-$; or, (iv) $\alpha_- = 0$ and $x_{-2}, x_{-1} \in \mathbf{R}^+$.

- in case $a > 1$ and $b < 0$, a solution $\{x_k\}_{k=-2}^{\infty}$ of (15) converges if, and only if, (i) $\alpha_+ \le 0$ and $x_{-2} = x_{-1} = \alpha_+$; (ii) $\alpha_- > 0$ and $x_{-2} = x_{-1} = \alpha_-$.

We may also make assertions on the limiting behaviors of subsequences $\{x_{2k}\}_{k=-1}^{\infty}$ and $\{x_{2k+1}\}_{k=-1}^{\infty}$ of solutions $\{x_k\}_{k=-2}^{\infty}$ of (15). These and others can be made by going through the previous results one by one, and are not listed here since they do not offer any new theoretical information.

Acknowledgement: The authors would like to thank the referee for several valuable comments and insightful suggestions. The work was supported by the National Natural Science Foundation of China (11161049)

References

[1] Q. Ge, C. M. Hou and S. S. Cheng. Complete asymptotic analysis of a nonlinear recurrence relation with threshold control. Advances in Difference Equations, Vol. 2010, Article ID 143849, 19 pages, 2010

[2] C. M. Hou, L. Han and S. S. Cheng. Complete asymptotic and bifurcation analysis for a difference equation with piecewise constant control. Advances in Difference Equations, Vol. 2010, Article ID 542073, 13 pages, 2010

[3] M.D. Bernardo, C. J. Budd, A. R. Champneys and P. Kowalczyk. Piecewise Smooth Dynamical Systesm, Springer, New York, 2008.

[4] H. Sedaghat. Nonlinear Difference Equations: Theory and Applications to Social Science Models, Kluwer Academic, Dordrecht, 2003.

Annual Review of Chaos Theory, Bifurcations and Dynamical Systems
Vol. 7, (2017) 41-55, www.arctbds.com.

Effect of Narrow Band Frequency Modulated Signal on Horseshoe Chaos in Nonlinearly Damped Duffing-vander Pol Oscillator

M.V. Sethumeenakshi
Department of Mathematics, St.Xavier's College, Palayamkottai-627 002, Tamilnadu, India.
e-mail: sethumeenakshi91@gmail.com

S. Athisayanathan
Department of Mathematics, St.Xavier's College, Palayamkottai-627 002, Tamilnadu, India.
e-mail: athisayanathan@yahoo.co.in

V. Chinnathambi
Department of Physics, Sri K.G.S. Arts College, Srivaikuntam-628 619, Tamilnadu, India.
e-mail: veerchinnathambi@gmail.com

S. Rajasekar
School of Physics, Bharathidasan Uuniversity, Thiruchirapalli-620 024, Tamilnadu, India.
e-mail: rajasekar@cnld.bdu.ac.in

Abstract: This paper invsetigates both analytically and numerically the effect of narrow band frequency modulated (NBFM) signal on horseshoe chaos in nonlinearly damped Duffing-vander Pol oscillator (DVP) system. Using the Melnikov analytical method, we obtain the threshold condition for the onset of horseshoe chaos. Threshold curves are drawn in various parameters spaces. We identify the regions of horseshoe chaos in various parameters spaces and bring out the effect of NBFM signal in DVP system. We illustrate that by varying the parameters f, g, p, one can suppress or enhance horseshoe chaos. We confirm the analytical results by the numerical tools such as computation of stable and unstable manifolds of saddle and threshold curves.

Keywords: Duffing-vander Pol oscillator, Nonlinear damping, NBFM signal, Horseshoe chaos, Melnikov method.

Manuscript accepted April 10, 2017.

1 Introduction

Over the past decades, a large number of analytical, numerical and experimental studies have been carried out on linearly damped nonlinear oscillator systems with an effort to understand the various features associated with the occurrence of chaotic behaviour [1-10]. Recently there have been attempts to study the effect of external periodic forces in certain nonlinearly damped nonlinear systems [11-25].

Horseshoe is the occurrence of transverse intersections of stable and unstable manifolds of a saddle fixed point in the Poincaré map and is a global phenomenon. In general, the existence of horseshoe does not imply that typical trajectories will be asymptotically chaotic. However the orbits created by the horseshoe mechanism display an extremely sensitive dependence on initial conditions and possibly exhibit either a chaotic transient before settling to stable orbits or strange attractor. Its appearance can be predicted analytically employing the Melnikov technique. Recently this method has been applied to certain nonlinear systems [5-11,13-19]. Nonlinearly damped Duffing-vander pol (DVP) oscillator under the influence of narrow band frequency modulated (NBFM) signal considered in the present paper is of the form

$$\ddot{x} + \gamma\, \dot{x}\, (1 - x^2)|\dot{x}|^{p-1} - \alpha^2 x + \beta x^3 = f(\cos\omega t - g \sin\Omega t \sin\omega t) \tag{1}$$

where $\gamma > 0$, $\alpha, \beta, \omega, \Omega$, p and f are constant parameters. DVP oscillator equation (Eq.1) serves as a basic model for self excited oscillations in Physics, Engineering, Electronics, Biology, Neurology and many other disciplines [1-8]. Recently the NBFM signal has been applied to certain nonlinear systems to investigate some nonlinear phenomena such as homoclinic bifurcations, stochastic and vibrational resonances etc. [26-29]. Our objective here is to explore the effect of NBFM signal on horseshoe chaos in Eq.(1) using both analytical and numerical techniques. In our present analysis, we use Melnikov analytical method to study the influence of NBFM signal on homoclinic orbits in Eq.(1).

2 Analytical results

In order to apply the Melnikov method to Eq.(1) we consider the system

$$\dot{x} = y \tag{2a}$$

$$\dot{y} = \alpha^2 x + \beta x^3 + \epsilon[\gamma\, (1 - x^2) y|y|^{p-1} + f(\cos\omega t - g \sin\Omega t \sin\omega t)] \tag{2b}$$

where ϵ is a small parameter. The unperturbed part of the system (Eq.2) with $\epsilon = 0$ has one saddle point $(x^*, y^*) = (0, 0)$ and two center type fixed points $(x^*, y^*) = (\pm\frac{\alpha}{\sqrt{\beta}}, 0)$. The two homoclinic orbits connecting the saddle to itself are given by

$$W^{\pm}(x_h(\tau), y_h(\tau)) = (\pm\alpha\sqrt{\frac{2}{\beta}}\, \mathrm{sech}\alpha\tau, \mp\alpha^2\sqrt{\frac{2}{\beta}}\, \mathrm{sech}\alpha\tau\, \tanh\alpha\tau), \qquad \tau = t - t_0 \tag{3}$$

The Melnikov theory [1, 2, 30] allows us to calculate the Melnikov function $M(t_0)$ for a classes of perturbed system for which homoclinic or heteroclinic orbit is known either analytically or numerically. $M(t_0)$ is proportional to the distance between the stable manifold

(W_s) and unstable manifold (W_u) of a saddle. When the stable and unstable manifolds are separated then the sign of $M(t_0)$ always remains same. $M(t_0)$ oscillates when W_s and W_u intersects transversely (horseshoe dynamics). The occurrence of transverse intersections implies the Poincaré map of the system has the so called *horseshoe chaos.*

From Eq.(2), the Melnikov function is worked out to be

$$M^{\pm}(t_0) = -\gamma \int_{-\infty}^{+\infty} |y_h|^{p+1} \left(1 - x_h^2\right)\ d\tau + f \int_{-\infty}^{+\infty} y_h \cos\omega(\tau + t_0)\ d\tau$$
$$-\frac{fg}{2} \int_{-\infty}^{+\infty} y_h \cos(\Omega - \omega)(\tau + t_0)\ d\tau + \frac{fg}{2} \int_{-\infty}^{+\infty} y_h \cos(\Omega + \omega)(\tau + t_0)\ d\tau \qquad (4)$$

Let $\omega_1 = (\Omega - \omega)$, $\omega_2 = (\Omega + \omega)$ and $G_1 = fg/2$

$\therefore$ the Eq.(4) becomes,

$$M^{\pm}(t_0) = -\gamma \int_{-\infty}^{+\infty} |y_h|^{p+1} \left(1 - x_h^2\right)\ d\tau + f \int_{-\infty}^{+\infty} y_h \cos\omega(\tau + t_0)\ d\tau$$
$$-G_1 \int_{-\infty}^{+\infty} y_h \cos\omega_1(\tau + t_0)\ d\tau + G_1 \int_{-\infty}^{+\infty} y_h \cos\omega_2(\tau + t_0)\ d\tau \qquad (5)$$
$$= \quad I_1 \quad + \quad I_2 \quad + \quad I_3 \quad + \quad I_4$$

(i) Evaluation of I_1

From Eq.(5), we have

$$I_1 \;=\; -\gamma \int_{-\infty}^{\infty} |y_h|^{p+1}\ (1 - x_h^2)\, d\tau$$

$$= \; -\gamma \int_{-\infty}^{\infty} |\, y_h\,|^{p+1}\ d\tau + \gamma \int_{-\infty}^{\infty} |\, y_h\,|^{p+1}\, x_h^2\, d\tau$$
$$= \qquad\qquad I_{11} \qquad + \qquad I_{12}$$

The evaluation of the integrals I_{11} and I_{12} gives the following results.

$$I_{11} = -\gamma(\alpha^2)^{p+\frac{1}{2}} \left(\frac{2}{\beta}\right)^{\frac{p+1}{2}} B\left[\frac{p+2}{2}, \frac{p+1}{2}\right]$$
$$I_{12} = \gamma(\alpha^2)^{p+\frac{3}{2}} \left(\frac{2}{\beta}\right)^{\frac{p+3}{2}} B\left[\frac{p+2}{2}, \frac{p+3}{2}\right]$$

Therefore,

$$I_1 = -\gamma(\alpha^2)^{p+\frac{1}{2}} \left(\frac{2}{\beta}\right)^{\frac{p+1}{2}} B\left[\frac{p+2}{2}, \frac{p+1}{2}\right] + \gamma(\alpha^2)^{p+\frac{3}{2}} \left(\frac{2}{\beta}\right)^{\frac{p+3}{2}} B\left[\frac{p+2}{2}, \frac{p+3}{2}\right] \qquad (6)$$

where $B(m,n)$ is the Euler Beta function which can be easily evaluated in terms of the Euler Gamma function. The relation connecting the Beta and Gamma function is

$$B(m,n) = \frac{\Gamma(m)\Gamma(n)}{\Gamma(m+n)} \tag{7}$$

where $\Gamma(m)$ denotes the Euler Gamma function

$$\Gamma(n) = \int_0^\infty e^{-x}x^{n-1}dx, \qquad n > 0 \tag{8}$$

(ii) Evaluation of I_2

From Eq.(5) we have,

$$\begin{aligned} I_2 &= f\int_{-\infty}^{\infty} y_h \cos\omega(\tau+t_0)\, d\tau \\ &= f\int_{-\infty}^{\infty} y_h(\cos\omega\tau\cos\omega t_0 - \sin\omega\tau\sin\omega t_0)\, d\tau \\ &= f\cos\omega t_0\int_{-\infty}^{\infty} y_h\cos\omega\tau d\tau - f\sin\omega t_0\int_{-\infty}^{\infty} y_h\sin\omega\tau d\tau \\ &= \qquad I_{21} \qquad + \qquad I_{22} \end{aligned}$$

After the evaluation of the integral I_{21}, the integral value of $I_{21} = 0$. The value of integral I_{22} is worked out to be

$$\begin{aligned} I_{22} &= \pm f\sin\omega t_0 \int_{-\infty}^{\infty} \alpha^2\sqrt{\frac{2}{\beta}}\,\text{sech}\alpha\tau\tanh\alpha\tau\sin\omega\tau d\tau \\ &= \pm\sqrt{\frac{2}{\beta}} f\pi\omega\ \text{sech}\ \left[\frac{\pi\omega}{2\alpha}\right]\sin\omega t_0 \end{aligned}$$

Therefore,

$$I_2 = \pm\sqrt{\frac{2}{\beta}} f\pi\omega\ \text{sech}\ \left[\frac{\pi\omega}{2\alpha}\right]\sin\omega t_0 \tag{9}$$

(iii) Evaluation of I_3

From Eq.(5) we have,

$$\begin{aligned} I_3 &= -G_1\int_{-\infty}^{\infty} y_h\cos\omega_1(\tau+t_0)\, d\tau \\ &= -G_1\int_{-\infty}^{\infty} y_h(\cos\omega_1\tau\cos\omega_1 t_0 - \sin\omega_1\tau\sin\omega_1 t_0)\, d\tau \\ &= -G_1\int_{-\infty}^{\infty} y_h\cos\omega_1\tau\cos\omega_1 t_0 d\tau + G_1\int_{-\infty}^{\infty} y_h\sin\omega_1\tau\sin\omega_1 t_0 d\tau \\ &= \qquad I_{31} \qquad + \qquad I_{32} \end{aligned}$$

The integral value of I_{31} is zero. The value of integral I_{32} is worked out to be

$$\begin{aligned} I_{32} &= G_1 \int_{-\infty}^{\infty} y_h \sin\omega_1\tau \sin\omega_1 t_0 d\tau \\ I_{32} &= -G_1 \sin\omega_1 t_0 \int_{-\infty}^{\infty} \alpha^2 \sqrt{\frac{2}{\beta}} \text{sech}\alpha\tau \tanh\alpha\tau \sin\omega_1\tau d\tau \\ &= \mp G_1 \sqrt{\frac{2}{\beta}} \pi\omega_1 \text{ sech}\left[\frac{\pi\omega_1}{2\alpha}\right] \sin\omega_1 t_0 \end{aligned}$$

Therefore,

$$I_3 = \mp G_1 \sqrt{\frac{2}{\beta}} \pi\omega_1 \text{ sech}\left[\frac{\pi\omega_1}{2\alpha}\right] \sin\omega_1 t_0 \tag{10}$$

(iv) Evaluation of I_4

Like the evaluation of I_3, the integral value of I_4 is obtained as

$$I_4 = \pm G_1 \sqrt{\frac{2}{\beta}} \pi\omega_2 \text{ sech}\left[\frac{\pi\omega_2}{2\alpha}\right] \sin\omega_2 t_0 \tag{11}$$

Therefore, Eq.(5) becomes

$$M^{\pm}(t_0) = A + B \pm C\ f \sin\omega t_0 \pm D\ G_1 \sin\omega_1 t_0 \pm E\ G_1 \sin\omega_2 t_0 \tag{12a}$$

where

$$A = -\gamma(\alpha^2)^{p+\frac{1}{2}} \left[\frac{2}{\beta}\right]^{\frac{p+1}{2}} B\left[\frac{p+2}{2}, \frac{p+1}{2}\right] \tag{12b}$$

$$B = \gamma(\alpha^2)^{p+\frac{3}{2}} \left[\frac{2}{\beta}\right]^{\frac{p+3}{2}} B\left[\frac{p+2}{2}, \frac{p+3}{2}\right] \tag{12c}$$

$$C = \sqrt{\frac{2}{\beta}}\ \pi\omega \text{ sech}\left[\frac{\pi\omega}{2\alpha}\right] \tag{12d}$$

$$D = -\sqrt{\frac{2}{\beta}}\ \pi(\Omega-\omega) \text{ sech}\left[\frac{\pi(\Omega-\omega)}{2\alpha}\right] \tag{12e}$$

$$E = \sqrt{\frac{2}{\beta}}\ \pi(\Omega+\omega) \text{ sech}\left[\frac{\pi(\Omega+\omega)}{2\alpha}\right] \tag{12f}$$

3 Numerical results

In this section we investigate the effect of NBFM signal on horseshoe chaos both analytically and numerically in the system (Eq.2) with the frequencies $\Omega = \omega$ and $\Omega \neq \omega$ cases respectively.

3.1 Effect of NBFM signal on horseshoe chaos for $G_1 = 0$ and $\Omega = \omega$

For $G_1 = 0$ and $\omega = \Omega$, the Eq.(12) becomes,

$$M^{\pm}(t_0) = A + B \pm C\, f \sin \omega t_0 \tag{13a}$$

The necessary condition for the occurrence of horseshoe chaos is

$$| f | \geq | f_m | = \gamma \left(\frac{2}{\beta}\right)^{\frac{p}{2}} \frac{(\alpha^2)^{p+\frac{1}{2}}}{\pi\Omega} \left\{ B\left[\frac{p+2}{2}, \frac{p+1}{2}\right] - \frac{2}{\beta}\alpha^2\, B\left[\frac{p+2}{2}, \frac{p+1}{2}\right] \right\} \cosh\left(\frac{\pi\omega}{2\alpha}\right) \tag{13b}$$

The sufficient condition requires the existence of simple zeros of $M(t_0)$. Equality sign in Eq.13(b) corresponds to tangential intersections. In Fig.1, we plotted the threshold curve for horseshoe chaos in the $(f, \Omega(=\omega))$ plane for $\alpha = 1.0, \beta = 5.0, \gamma = 0.4$ and various p values.

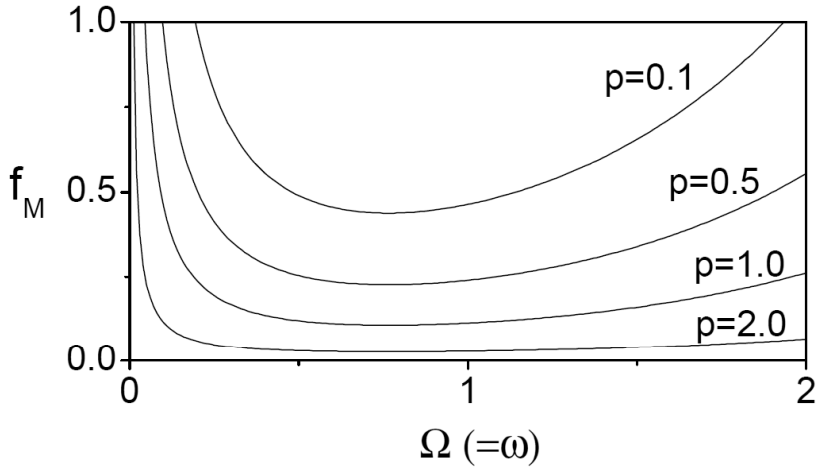

Figure 1: Melnikov threshold curves for horseshoe chaos in the $(f, \Omega(=\omega))$ plane for the system (Eq.2) driven by NBFM signal for various p values. The values of the other parameters in Eq.(2) are $\alpha = 1.0, \beta = 5.0, \gamma = 0.4$ and $g = 0.0$.

Below the curve, no transverse intersections of stable $(W_s^{\pm})$ and unstable $(W_u^{\pm})$ manifolds of the saddle occurs and above the curve, transverse intersections of stable $(W_s^{\pm})$ and unstable $(W_u^{\pm})$ occurs. Just above the Melnikov threshold curve, onset of cross-well chaos is expected. We have verified the analytical prediction by directly integrating the Eq.(2) using the fourth-order Runge-Kutta method. As an example, Fig.2 shows the part of the numerically computed stable and unstable orbits in the Poincaré map for $f = 0.1$ and $f = 0.3$ with $p = 0.5$ and $\Omega = \omega = 1$. The unstable manifolds are obtained by integrating the Eq.(1) in the forward time for a set of 900 initial conditions chosen around the perturbed saddle point. The stable manifolds are obtained by integrating the Eq.(1) in reverse time. For $f = 0.1$ the two orbits are well separated. In this parametric regime,

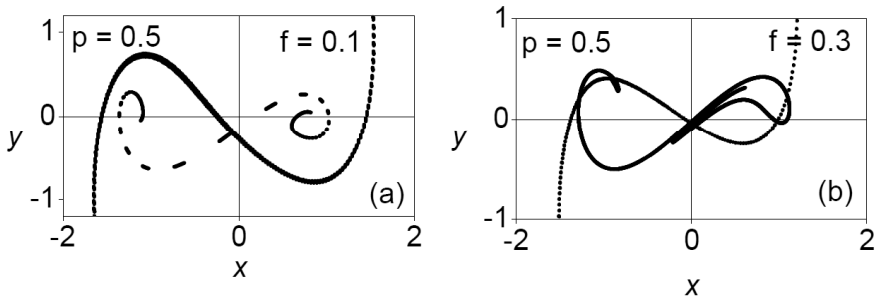

Figure 2: Numerically computed stable and unstable manifolds of the saddle fixed point of the system (Eq.2) driven by NBFM signal for (a) $f = 0.1$ and (b) $f = 0.3$ with $p = 0.5$. The values of the other parameters in Eq.(2) are $\alpha = 1.0, \beta = 5.0, \gamma = 0.4$ and $\Omega = \omega = 1.0$.

one may expect periodic behaviour. For $f = 0.3$ we can clearly notice transverse intersections of orbits at three places (Fig.2(b)). In this region, it is possible to have either asymptotic chaos or transient chaos followed by asymptotic periodic behaviour.

In order to know the nature of the attractors of the system near the horseshoe threshold value we have further numerically studied the Eq.(1) and the onset of cross-well chaos. Fig.3 shows the bifurcation and the corresponding maximal Lyapunov exponent diagrams for $p = 1.0$ and $p = 2.0$ with $g = 0.0$. From Fig.3, the onset of cross-well chaos are found to occur at $f = 0.12334$ for $p = 1.0$ and $f = 0.09674$ for $p = 2.0$. The analytically predicted Melnikov threshold values (f_M) for $p = 1.0$ and $p = 2.0$ are 0.125 and 0.09754. The analytical prediction is in good agreement with the actual numerical analysis of the system.

3.2 Effect of NBFM signal on horseshoe chaos for $G_1 \neq 0$ and $\Omega = \omega$

First we consider the effect of NBFM signal on horseshoe chaos in the system (Eq.2) by fixing the value of g and thereby varying f. For $\Omega = \omega$, we have D=0 in Eq.12(e) and the Melnikov function given by Eq.12(a) becomes,

$$M^{\pm}(t_0) = A + B \pm C\, f \sin\omega t_0 \pm E\, G_1 \sin 2\omega t_0 \tag{14a}$$

The necessary condition for the occurrence of horseshoe chaos is

$$f \geq f_M^{\pm} = (A + B \pm EG_1) \,/\, C \tag{14b}$$

(or)

$$f \leq f_M^{\prime\pm} = (-A - B \mp EG_1) \,/\, C \tag{14c}$$

where the superscripts sign $'+'$ and $'-'$ correspond to the homoclinic orbits W^+ and W^- respectively.

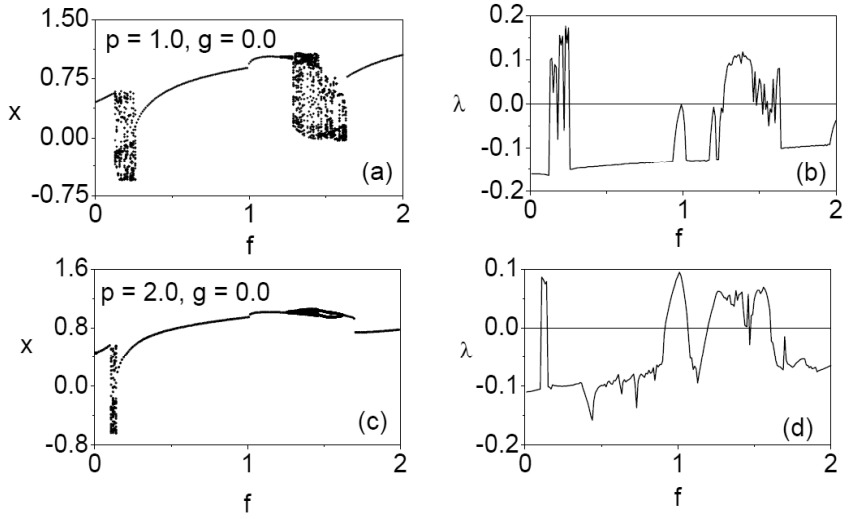

Figure 3: Bifurcation and the corresponding maximal Lyapunov exponent diagrams for the system (Eq.1) driven by NBFM signal for (a-b) $p = 1.0$ and (c-d) $p = 2.0$. The values of the other parameters in Eq.(1) are $\alpha = 1.0, \beta = 5.0, \gamma = 0.4, g = 0.0$ and $\Omega = \omega = 1.0$.

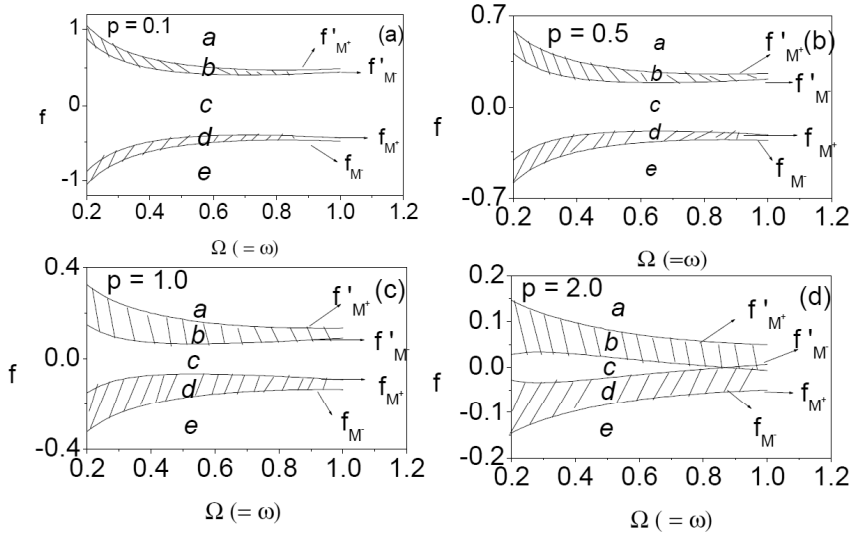

Figure 4: Melnikov threshold curves for horseshoe chaos in the $(f, \Omega(=\omega))$ plane for the system (Eq.2) driven by NBFM signal for four p values. The values of the other parameters in Eq.(2) are $\alpha = 1.0, \beta = 5.0, \gamma = 0.4$ and $g = 0.1$.

Figure 4 shows the threshold curves for the occurrence of horseshoe chaos in the $(f, \Omega(=\omega))$ plane for $\Omega = \omega$, $\alpha = 1.0, \beta = 5.0, \gamma = 0.4$, $g = 0.1$ and various p values. In the regions a and e both $M^+(t_0)$ and $M^-(t_0)$ change sign and the transverse intersections of stable and unstable parts of W^+ and W^- occur. $M^+(t_0)$ alone changes sign in the region b and hence transverse intersections of orbits of W^+ occur. In region c, no transverse intersections of both stable and unstable manifolds of saddle occur. In the region d, transverse intersections of (W_u^-) and unstable (W_s^-) alone take place. We verified this by direct simulation of the system (Eq.2). As an example, Fig.5 shows the part of stable and unstable orbits in the Poincaré map for four values of f chosen in the regions a, b, c and d with $\Omega = \omega = 1$, $g = 0.1$ and $p = 2.0$. Transverse intersections

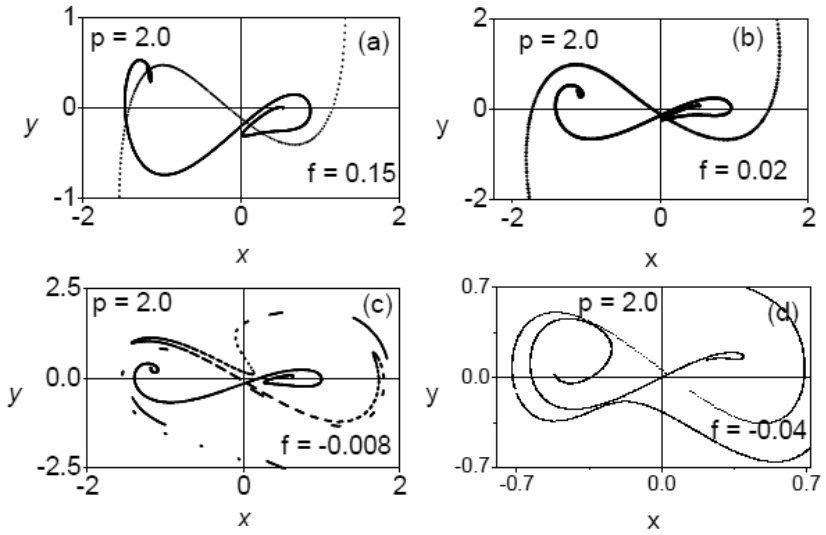

Figure 5: Numerically computed stable and unstable manifolds of the saddle fixed point of the system (Eq.2) driven by NBFM signal for four values of f chosen in the regions a, b, c and d with $p = 2.0$ and $g = 0.1$. The values of the other parameters in Eq.(2) are $\alpha = 1.0, \beta = 5.0, \gamma = 0.4$ and $\Omega = \omega = 1.0$.

of stable and unstable branches of both the homoclinic orbits $W_s^{\pm}$ and $W_u^{\pm}$ can be clearly seen in Fig.5(a) for $f = 0.15$ which falls in the region a. In Fig.5(b) we see the intersections of W_s^+ and W_u^+ orbits alone at one place for $f = 0.02$ (region b) while for $f = -0.008$ (region c) no transverse intersection of orbits occur. This is shown in Fig.5(c). For $f = -0.04$ (Fig.5(d)) which corresponds to the region d, branches W_s^- and W_u^- alone intersect.

Next we analyze the effect of NBFM signal on horseshoe chaos for a fixed value of f and thereby varying g. The necessary condition on g for $M(t_0)$ to change sign is

$$G_1 \geq G_{1M}^{\pm} = (A + B \pm Cf) / E \tag{15a}$$

$$G_1 \leq G_{1M}^{'\pm} = (-A - B \mp Cf) / E \tag{15b}$$

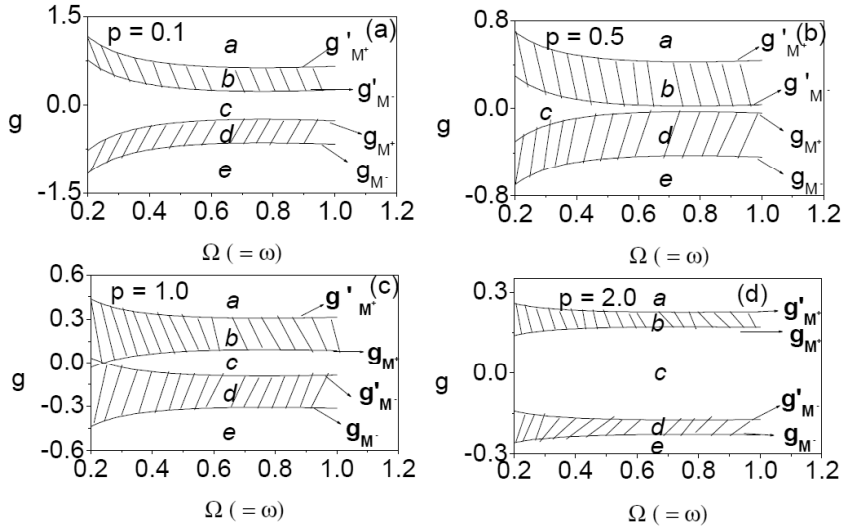

Figure 6: Melnikov threshold curves for horseshoe chaos in the $(g, \Omega(=\omega))$ plane for the system (Eq.2) driven by NBFM signal for four p values. The values of the other parameters in Eq.(2) are $\alpha = 1.0, \beta = 5.0, \gamma = 0.4$, and $f = 0.2$.

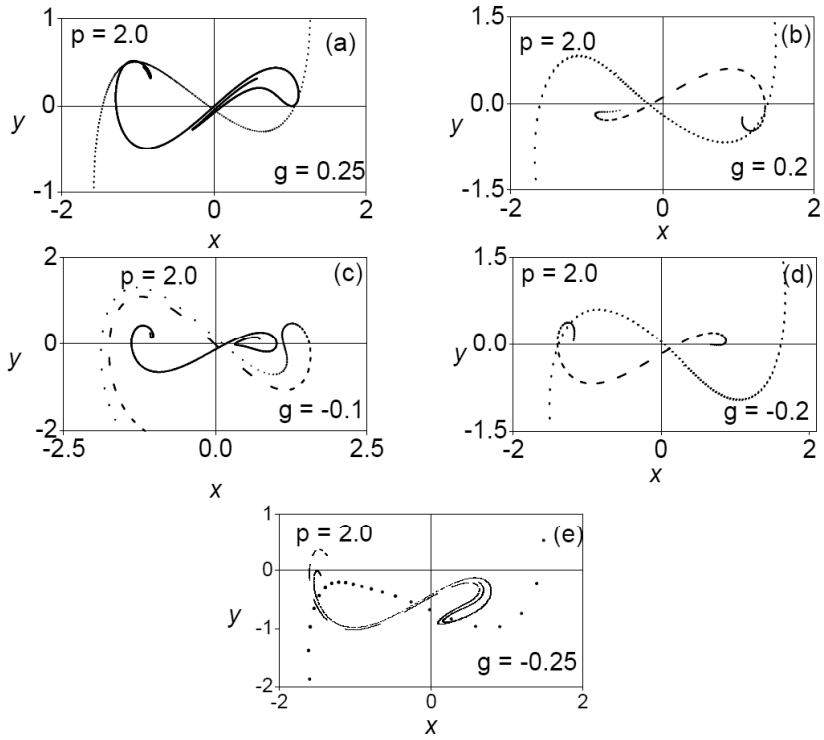

Figure 7: Numerically computed stable and unstable manifolds of the saddle fixed point of the system (Eq.2) driven by NBFM signal for five values of g with $p = 2.0$. The values of the other parameters in Eq.(2) are $\alpha = 1.0, \beta = 5.0, \gamma = 0.4$ $f = 0.2$ and $\Omega = \omega = 1.0$.

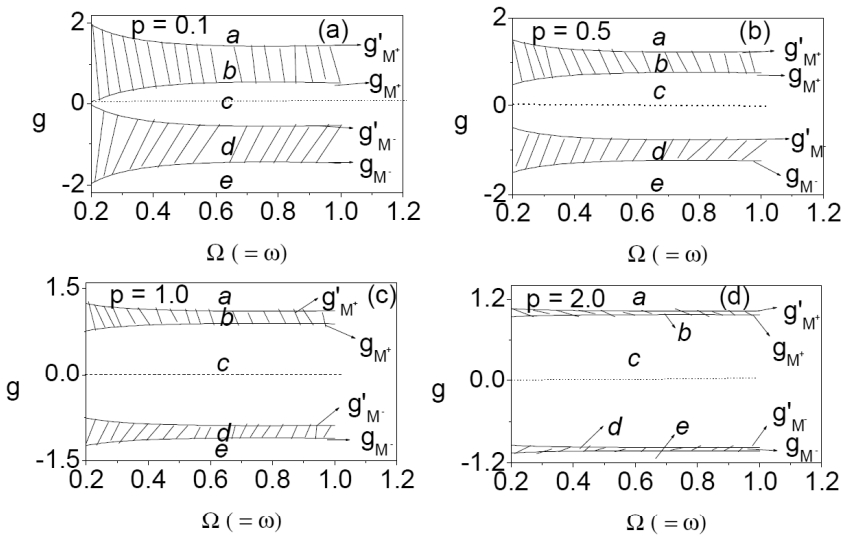

Figure 8: Melnikov threshold curves for horseshoe chaos in the $(g, \Omega(=\omega))$ plane for the system (Eq.2) driven by NBFM signal for four p values. The values of the other parameters in Eq.(2) are $\alpha = 1.0, \beta = 5.0, \gamma = 0.4$ and $f = 1.0$.

Figure 6 shows the Melnikov threshold curves for horseshoe chaos in the $(g, \Omega(=\omega))$ plane for $f = 0.2$ with four values of p. For $p = 2.0$, we have verified the above analytical results by direct simulation of the system (Eq.2). Figure 7 shows the part of stable and unstable orbits in the Poincaré map for five values of g chosen in the regions a, b, c, d and e with $\Omega = \omega = 1$ and $f = 0.2$. Then we fixed $f = 1.0$ above the threshold values for all the values of p with $g = 0.0$ and studied the effect of modulating term by varying g. Figure 8 shows the Melnikov threshold curves for $f = 1.0$. When $f = 1.0$ and $g = 0.0$ transverse intersections of stable and unstable manifolds of saddle occur for a range of ω (see Fig.1). This is represented by the straight line in Fig.8. When g is switched on even for small values of g, transverse intersections suddenly disappear. That is horseshoe chaos is suppressed. This occurs for a range of values of g.

3.3 Effect of NBFM signal on horseshoe chaos for $G_1 \neq 0$ and $\Omega \neq \omega$

In the previous section we studied the effect of NBFM signal on horseshoe chaos for the case of $\Omega = \omega$. In this section, we consider the case $\Omega \neq \omega$. For this case, we cannot write the necessary condition for the occurrence of horseshoe chaos similar to Eq.(14) or (15). However the occurrence of horseshoe chaos can be studied numerically measuring the time τ_M elapsed between the successive transverse intersection. τ_M can be determined from Eq.(12). Figure 9 shows the variation of $1/\tau_M^{\pm}$ versus f for $\omega = 1.0$, $\Omega = \sqrt{2}$, $\alpha = 1.0, \beta = 5.0, \gamma = 0.4$, $g = 0.1$ and four values of p. Continuous curves represent the inverse of first intersection time $1/\tau_M^{\pm}$ of stable and unstable branches of homoclinic

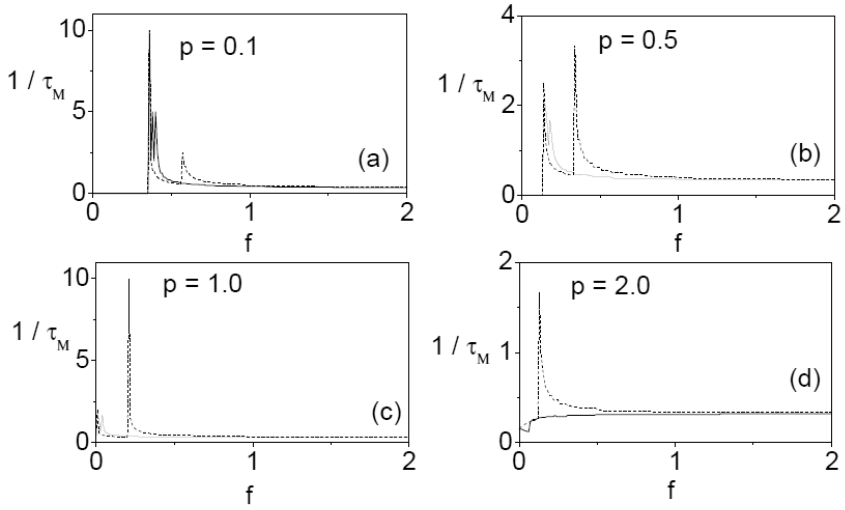

Figure 9: Variation of $1/\tau_M^{\pm}$ versus f for $g = 0.1$, $\omega = 1.0$, $\Omega = \sqrt{2}$ and four values of p. The values of the other parameters in Eq.(2) are $\alpha = 1.0, \beta = 5.0$ and $\gamma = 0.4$.

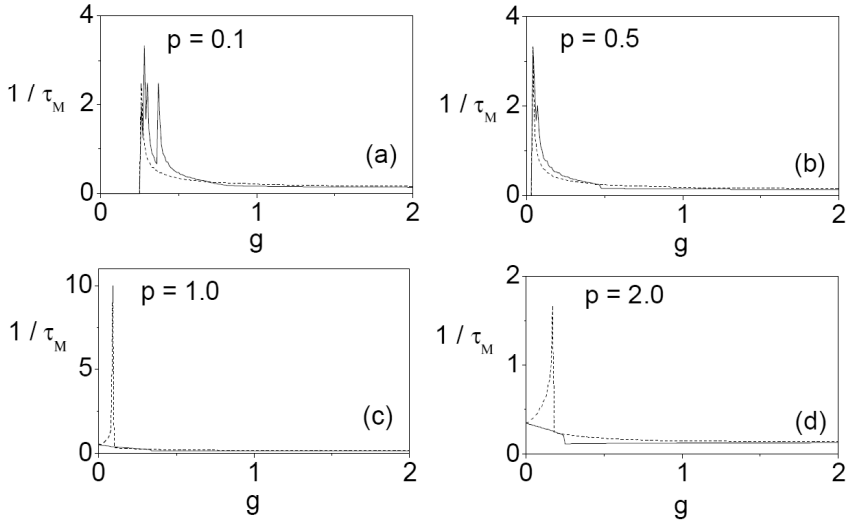

Figure 10: Variation of $1/\tau_M^{\pm}$ versus g for $f = 0.2$, $\omega = 1.0$, $\Omega = \sqrt{2}$ and four values of p. The values of the other parameters in Eq.(2) are $\alpha = 1.0, \beta = 5.0$ and $\gamma = 0.4$.

orbits W^+. Dashed curves correspond to the orbits of W^-. Horseshoe chaos does not occur when $1/\tau_M^{\pm}$ is zero and it occurs in the region when $1/\tau_M^{\pm} > 0$. In Fig.9, when the value of g is fixed at 0.1, $1/\tau_M^{\pm}$ are zero for $0 < f < 0.35792$ for $p = 0.1$ (Fig.9(a)), $0 < f < 0.13785$ for $p = 0.5$ (Fig.9(b)), $0 < f < 0.01935$ for $p = 1.0$ (Fig.9(c)) and hence no horseshoe chaos occurs in this interval of f. For the other values of f, $1/\tau_M^{\pm}$ are nonzero, that is, horseshoe chaos occurs. Figure 10 shows the plot of $1/\tau_M^{\pm}$ against g for $\alpha = 1.0, \beta = 5.0, \gamma = 0.4, f = 0.2, \omega = 1.0$ and $\Omega = \sqrt{2}$. In Fig.10, $1/\tau_M^{\pm}$ are zero for $0 < g < 0.25227$ for $p = 0.1$ (Fig.10(a)) and $0 < g < 0.03458$ for $p = 0.5$ (Fig.10(b)). For other values of g, $1/\tau_M^{\pm}$ are nonzero.

4 Conclusion

The study of the effect of NBFM signal on horseshoe chaos is carried out in nonlinearly damped DVP system (Eq.2). Both analytically and numerically we studied the effect of NBFM signal on horseshoe chaos in DVP system (Eq.2). Applying Melnikov analytical method we obtained the threshold condition for onset of horseshoe chaos, that is, transverse intersection of stable and unstable branches of homoclinic orbits. Threshold curves are drawn on different parameters spaces. We demonstrated the effect of the parameters f, g, Ω and p on the dynamics of the system (Eq.2).

When the damping exponent (p) increases from small values, the threshold value decreases for onset of horseshoe chaos. The introduction of nonlinear damping term affects the various nonlinear behaviours such as period doubling route to chaos, crises, threshold values for the horseshoe chaos etc. For typical parametric values, we have shown the suppression and enhancement of horseshoe chaos due to the effect of nonlinear damping and NBFM signal. Analytical prediction of horseshoe chaos is found to be in good agreement with numerical simulation of the system (Eq.2). In the present work, we studied the effect of NBFM signal on horseshoe chaos in system (Eq.2) with symmetric potential. It is important to study the effect of nonlinear damping and NBFM signal with three different asymmetric potentials . These will be investigated in future.

References

[1] J. Guckenheimer and P. Holmes, The Nonlinear Oscillations, Dynamical Systems and Bifurcations of Vector Fields, *(Springer, New York, 1983).*

[2] S. Wiggins, Introduction to Applied Nonlinear Dynamical Systems and Chaos, *(Springer, New York, 1990).*

[3] E. Ott, Chaos in Dynamical Systems, *(Cambridge University Press, New York, 1993).*

[4] M. Lakshmanan and S. Rajasekar, Nonlinear Dynamics: Integrability, Chaos and Patterns, *(Springer, Berlin, 2003).*

[5] S. Rajasekar, Controlling of Chaos by Weak Periodic Perturbations in DVP Oscillator, *Pramana J. of Physics*, 41, 295-309, 1993.

[6] Z. Zing, Z. Yang and T. Jiang, Complex Dynamics in DVP equation, *Chaos, Solitons and Fractals*, 27, 722-747, 2006.

[7] L. Ravisankar, V. Ravichandran and V. Chinnathambi, Prediction of Horseshoe Chaos in Duffing-vander Pol Oscillator Driven by Different Periodic Forces, *Int. J. of Eng. and Sci.*, 1(5), 17-25, 2012.

[8] S. Rajasekar, S. Parthasarathy and M. Lakshmanan, Prediction of Horseshoe Chaos in BVP and DVP Oscillators, *Chaos, Solitons and Fractals*, 2(3), 271-280, 1992.

[9] V. Ravichandran, V. Chinnathambi, S. Rajasekar and C.H. Lai, Effect of the Shape of Periodic Forces on Horseshoe Chaos in Duffing Oscillator, *arXiv: 0808 0406V1 [nlin.CD]*, 4 Aug 2008.

[10] V. Ravichandran, V. Chinnathambi and S. Rajasekar, Homoclinic Bifurcation and Chaos in Duffing Oscillator Driven by an Amplitude Modulated Force, *Physica A*, 376, 223-236, 2007.

[11] J.P. Baltanas, J.L. Trueba and M.A.F. Sanjuan, Energy Dissipation in a Nonlinearly Damped Duffing Oscillators, *Physica D*, 159, 22-34, 2001.

[12] S.J. Elliot, M. Ghandchi Tehrani and R.L. Langley, Nonlinear Damping and Quasi-Linear Modelling, *Phil. Frans. R. Soc. A*, 373, 20140402. http://dx.doi.org/10.1098/rsta.2014.0402 -30pp, 2015.

[13] Z.M. Ge and C.Y. Ou, Chaos in a Fractional Order Modified Duffing System, *Chaos, Solitons and Fractals*, 14, 262-291, 2007.

[14] J.L. Trueba, J. Rams and M.A.F Sanjuan, Analytical Estimates of the Effect of Nonlinear Damping in Some Nonlinear Oscillators, *Int. J. Bifur. and Chaos*, 10(9), 2257-2267, 2000.

[15] M. Borowice, G. Litak and A. Syta, Vibration of the Duffing Oscillator; Effect of Fractional Damping, *Shock and Vibration*, 14, 29-36, 2007.

[16] M.A.F. Sanjuan, The Effect of Nonlinear Damping on the Universal Escape Oscillator, *Int. J. of Bifur. and Chaos*, 9, 735-744, 1999.

[17] G. Litak, M. Borowiee and A. Syta, Vibration of Generalized Double-well DVP oscillator, *arXiv:nlin/0610052v1 [nlin.CD]*, 20 Oct 2006.

[18] M.V. Sethumeenakshi, S. Athisayanathan, V. Chinnathambi and S. Rajasekar, *Effect of Fractional Damping in Double-Well DVP Oscillator Driven by Different Sinusoidal Periodic Forces* , (Submitted for Publication, 2016).

[19] M.V. Sethumeenakshi, S. Athisayanathan, V. Chinnathambi and S. Rajasekar, Effect of Fractional Damping in Double-Well DVP oscillator Driven by Different Nonsinusoidal Periodic Forces, (Submitted for Publication, 2016).

[20] J. Padovan and J.T. Sawicki, Nonlinear Vibration of Fractional Damped Systems, *Nonlinear Dynamics*, 16, 321-336, 1998.

[21] R.E. Mickens, K.O. Oyedeji and S.A. Rucker, Analysis of the Simple Harmonic Oscillator with Fractional Damping, *J. Sound and Vib.*, 268, 839-842, 2003.

[22] L.J. Shen, H.K. Chen, J.H. Chen and L.M. Tam, Chaotic Dynamics of the Fractionally Damped Duffing Equation, *Chaos, Solitons and Fractals*, 31, 1203-1212, 2007.

[23] L. Cveticanin, Oscillator With Strong Quadratic Damping Force, *Publications de L'institute of Mathematique, Nouville Serie, Tome*, 85, 119-130, 2009.

[24] B. Ravindra and A.K. Mallik, Stability Analysis of a Nonlinearly Damped Duffing Oscillator, *J. Sound. Vib.*, 171, 708-716, 1994.

[25] B. Ravindra and A.K. Mallik, Role of Nonlinear Dissipation in Soft Duffing Oscillators, *Phys. Rev. E*, 49, 4950-4954, 1994.

[26] L. Ravisankar, V. Ravichandran, V. Chinnathambi and S. Rajasekar, Effect of Narrow Band Frequency Modulated Force on Horseshoe Chaos in Duffing-vander Pol Oscillator, *Int. J. of Sci. and Eng. Res.*, 48, 1155-1162, 2013.

[27] L. Ravisankar, V. Ravichandran, V. Chinnathambi and S. Rajasekar, Horseshoe Dynamics in Asymmetric Duffing-vander Pol Oscillator Driven by Narrow Band Frequency Modulated Force, *Chinese J. of Physics*, 52(3), 1026-1043, 2014.

[28] Y.C. Lai, Z. Liu, A. Nachman and L. Zhen, Suppression of Jamming in Excitable System by Aperiodic Stochastic Resonance, *Int. J. of. Bifur. and Chaos*, 14, 3519-3539, 2000.

[29] S. Guruparan, B. Ravindran Durai Nayagam, V. Ravichandran, V. Chinnathambi and S. Rajasekar, Vibrational Resonance in the Classical Morse Oscillator Driven by NBFM and WBFM Signals, *Journal of Pure Applied Chemical Research*, 5(3), 131-141, (2016).

[30] F.C Moon and G.X. Li, Fractal Basin Boundaries and Homoclinic Orbits for Periodic Motions in a Two-Well Potential, *Phys. Rev. Lett.*, 55, 1439-1442, 1985.